

Dilution refrigeration with multiple mixing chambers

Citation for published version (APA):

Coops, G. M. (1981). *Dilution refrigeration with multiple mixing chambers*. [Phd Thesis 1 (Research TU/e / Graduation TU/e), Applied Physics and Science Education]. Technische Hogeschool Eindhoven.
<https://doi.org/10.6100/IR36684>

DOI:

[10.6100/IR36684](https://doi.org/10.6100/IR36684)

Document status and date:

Published: 01/01/1981

Document Version:

Publisher's PDF, also known as Version of Record (includes final page, issue and volume numbers)

Please check the document version of this publication:

- A submitted manuscript is the version of the article upon submission and before peer-review. There can be important differences between the submitted version and the official published version of record. People interested in the research are advised to contact the author for the final version of the publication, or visit the DOI to the publisher's website.
- The final author version and the galley proof are versions of the publication after peer review.
- The final published version features the final layout of the paper including the volume, issue and page numbers.

[Link to publication](#)

General rights

Copyright and moral rights for the publications made accessible in the public portal are retained by the authors and/or other copyright owners and it is a condition of accessing publications that users recognise and abide by the legal requirements associated with these rights.

- Users may download and print one copy of any publication from the public portal for the purpose of private study or research.
- You may not further distribute the material or use it for any profit-making activity or commercial gain
- You may freely distribute the URL identifying the publication in the public portal.

If the publication is distributed under the terms of Article 25fa of the Dutch Copyright Act, indicated by the "Taverne" license above, please follow below link for the End User Agreement:

www.tue.nl/taverne

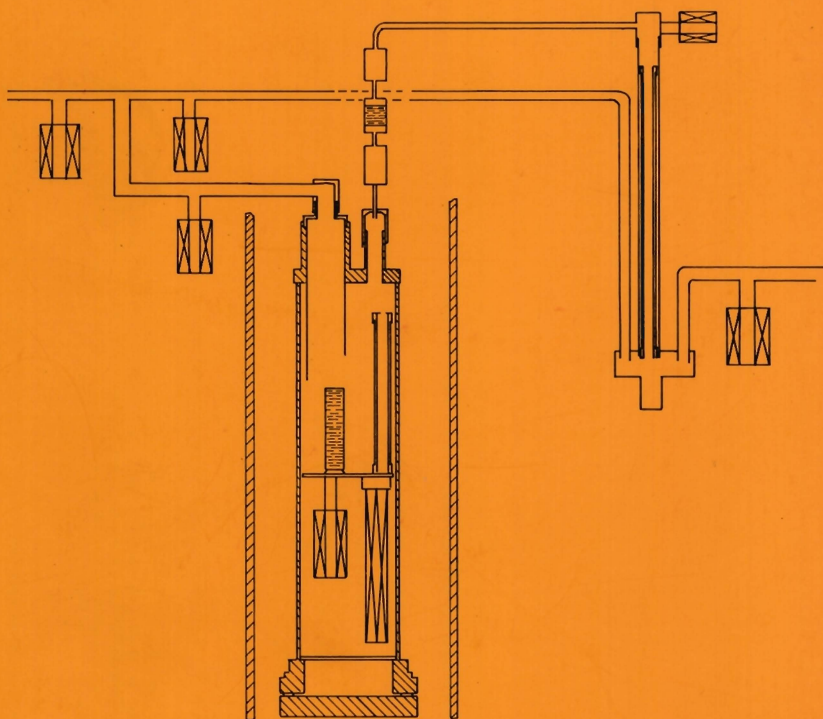
Take down policy

If you believe that this document breaches copyright please contact us at:

openaccess@tue.nl

providing details and we will investigate your claim.

DILUTION REFRIGERATION WITH MULTIPLE MIXING CHAMBERS



G. M. COOPS

DILUTION REFRIGERATION WITH MULTIPLE MIXING CHAMBERS

PROEFSCHRIFT

TER VERKRIJGING VAN DE GRAAD VAN DOCTOR IN DE
TECHNISCHE WETENSCHAPPEN AAN DE TECHNISCHE
HOGESCHOOL EINDHOVEN, OP GEZAG VAN DE
RECTOR MAGNIFICUS, PROF. IR. J. ERKELENS, VOOR
EEN COMMISSIE AANGEWEEZEN DOOR HET COLLEGE
VAN DEKANEN IN HET OPENBAAR TE VERDEDIGEN OP
VRIJDAG 12 JUNI 1981 TE 16.00 UUR

DOOR

GERARD MARINUS COOPS

GEBOREN TE 's-GRAVENHAGE

Dit proefschrift is goedgekeurd door de promotoren
Prof.dr. H.M. Gijsman en Prof.dr. R. de Bruyn Ouboter.
Co-promotor: Dr. A.Th.A.M. de Waele.

This investigation is part of the research program of the
"Stichting voor Fundamenteel Onderzoek der Materie (FOM)",
which is financially supported by the "Nederlandse Organisatie
voor Zuiver Wetenschappelijk Onderzoek (ZWO)".

Aan mijn ouders
Aan Wil

CONTENTS.

	<u>page</u>	
CHAPTER I	INTRODUCTION AND HISTORICAL SURVEY.	1
	1.1 Historical survey.	1
	1.2 The multiple mixing chamber.	2
	1.3 Contents.	3
	References.	4
CHAPTER II	THE PRINCIPLES OF DILUTION REFRIGERATION.	6
	2.1 Introduction.	6
	2.2 The ³ He circulating dilution refrigerator	6
	2.3 Enthalpy considerations.	10
	References.	13
CHAPTER III	THERMOMETRY.	14
	3.1 Introduction	14
	3.2 Resistance thermometry and the maximum allowable dissipation.	14
	3.3 CMN thermometry.	16
	3.4 Thermometry with partly dehydrated CMN.	18
	3.5 Dehydration and saturated vapour pressure of CMN.	21
	References.	23
CHAPTER IV	THE DESIGN OF TUBES AND HEAT EXCHANGERS AND THE CONSEQUENCE ON THE MINIMUM TEMPERATURE OF A DILUTION REFRIGERATOR.	24
	4.1 Introduction	24
	4.2 Design considerations concerning tubes.	24
	4.2.1 The concentrated side.	25
	4.2.2 The dilute side.	26
	4.3 Design considerations for heat exchangers.	27
	Conclusions.	34
	References.	35
CHAPTER V	THE DILUTION REFRIGERATOR WITH A CIRCULATION RATE OF 2.5 MMOL/S.	36
	5.1 Introduction.	36

CONTENTS (continued 1)

5.2	General description of the system.	36
5.3	Heat exchange in the 4 K - 80 K region.	37
5.4	The liquid helium consumption of the 1 K plate.	39
5.5	Limitation of the ^3He velocity by the still orifice.	41
5.6	The construction and performance of the heat exchangers.	44
	References.	47
CHAPTER VI	THE MULTIPLE MIXING CHAMBER (THEORY).	48
6.1	Introduction.	48
6.2.1	The double mixing chamber.	48
6.2.2	The value of Z_2 .	49
6.2.3	Dimensionless form of the equations.	50
6.2.4	Height of the mixing chambers.	52
6.2.5	The dilute exit temperature of a double mixing chamber system.	55
6.3	The construction of a DMC system.	56
6.4	Comparison between a single and a multiple mixing chamber system.	58
6.5	The triple mixing chamber.	60
	Conclusions.	62
	References.	63
CHAPTER VII	MEASUREMENTS ON MULTIPLE MIXING CHAMBER SYSTEMS	64
7.1	Introduction.	64
7.2	The experimental set-up.	64
7.3	The experimental procedure.	66
7.4	Cooling power measurements.	66
7.5	The t_2 vs. q_2 measurements.	70
7.6	The t_1 vs. q_2 measurements.	72
7.7	The dependence of A_1 and t_2 on T_1 .	73
7.8	The dependence of the minimum temperature on Z_1 .	74

CONTENTS (continued 2)

7.9	The dependence of the minimum temperature on the flow rate.	76
7.10	Measurements of Δh .	76
7.11	The relation between the temperature of MCl and the temperature of the exit of the impedance.	78
7.12	The entrance and exit temperature of a DMC and a SMC.	79
	Conclusions.	80
	References.	81
	SUMMARY.	82
	SAMENVATTING.	84
	SOME QUANTITIES USED IN THIS THESIS.	87
	LIST OF FREQUENTLY USED SYMBOLS.	88
	DANKWOORD.	90
	CURRICULUM VITAE.	91

CHAPTER I.

INTRODUCTION AND HISTORICAL SURVEY.

1.1 Historical survey.

Before 1965 the only known method for cooling below 0.3 K was adiabatic demagnetisation. In this year the first successful operation of a dilution refrigerator was reported by Das, de Bruyn Ouboter and Taconis (1965). This refrigerator, based on the cooling achieved by dilution of ^3He in ^4He , had a rapid development since that time. The technique was originally proposed by London et al. (1951, 1962).

The separation of the phases of a $^3\text{He} - ^4\text{He}$ mixture below 870 mK, discovered by Walters et al. (1956), plays a crucial role in the dilution refrigerator, especially because ^3He has a finite solubility in ^4He near absolute zero temperature as discovered by Edwards et al. (1965).

After the experiments of Das et al. (1965) more research was done by Hall (1966), Neganov (1968) and Wheatley (1968,1971).

Comprehensive treatments of the principles and methods were reported by Wheatley et al. (1968) and a description of the thermodynamic properties of $^3\text{He} - ^4\text{He}$ mixtures was given by Radebaugh (1967).

The research on the efficiency of heat exchangers which, constitute an essential part of the dilution refrigerator, has been subject of investigations (Siegwarth, 1972; Staas, 1974). The Kapitza resistance, a thermal resistance due to the phonon mismatch between the helium liquids and solids, hampers the heat exchange at low temperatures and this demands large surfaces areas. Niinikoski (1971) introduced a new type of heat exchanger leaving an open channel for flowing liquids. Frossati (1977) extended this idea and reported the lowest temperature ever reached in continuous mode.

At the lowest temperatures also the dimensions of the tubes become important (Wheatley, 1968; De Waele, 1977; Van Haeringen, 1979a, 1979b, 1980).

During these developments the need was felt to avoid the Kapitza resistance. New concepts were introduced.

Methods circulating ^4He instead of ^3He were proposed by Taconis et al. (1971, 1978). A further improvement in ^4He circulating machines is the ^3He and ^4He circulating machine which was developed by Staas et al. (1975) at Philips Laboratories and by Frossati et al. (1975) in Grenoble. Temperatures down to 4 mK are reported.

Another alternative method, the multiple mixing chamber, was introduced by De Waele, Gijsman and Reekers (1976). They reported in 1976 the successful operation of a double mixing chamber. In 1977 the minimum temperature was 3 mK by using a triple mixing chamber (De Waele, 1977).

1.2 The multiple mixing chamber.

Because the multiple mixing chamber is the central theme of this thesis we will treat it in more detail here. In a double mixing chamber, a special case of a multiple mixing chamber, the concentrated ^3He is precooled in the first mixing chamber, before it enters the second mixing chamber. In the triple mixing chamber the precooling takes place in the first and second mixing chamber successively. The use of a multiple mixing chamber has many advantages (Coops, 1979). The volume of the first mixing chamber can be very small. In this way a relatively small amount of ^3He is necessary to reach the same temperature as a conventional dilution unit. Adding a mixing chamber to an existing system lowers the temperature and enlarges the cooling power.

As an example we will give the measured minimum temperature, the cooling power at a certain temperature for two flow rates of a DMC and a SMC system with the same exchange area in the heat exchangers.

\dot{n}_i (mmol/s)		SMC	DMC
1.0	T_{\min} (mK)	19	12.5
	$\dot{Q}(20 \text{ mK})$ (W)	5.7	16
0.5	T_{\min} (mK)	13.5	7.8
	$\dot{Q}(10 \text{ mK})$ (W)	no cooling power	1.4

Table 1.1 The comparison between a single mixing chamber (SMC) and a double mixing chamber (DMC) for two different flow rates.

The minimum temperature is lower and the cooling power is larger in both cases. We also compare the triple mixing chamber (TMC) with a single mixing chamber and we observe the same improvement.

\dot{n}_1 ($\mu\text{mol/s}$)		SMC	TMC
28	T_{min} (mK)	9.4	5
	\dot{Q} (10 mK) (nW)	50	250

Table 1.2. The comparison between a SMC and a TMC.

The multiple mixing chamber is a reliable tool to lower the minimum temperature without using more surface area in the heat exchangers (more ^3He) and increases the cooling power of an existing dilution refrigerator.

As has been noted before, the minimum temperature reached in our laboratory was 3 mK by using a triple mixing chamber.

1.3 Contents.

In this thesis we will only deal with ^3He circulating machines. Chapter II deals with the principles of the conventional dilution refrigerator. Some important equations, useful for other chapters, will be derived.

To measure the relevant parameters of the dilution unit it is important to have a well developed thermometry. Chapter III describes the research done on resistance and CMN thermometry. The design of tubes and heat exchangers is discussed in chapter IV. It will be shown that to obtain the lowest temperatures large machines are necessary. Since originally we had a small dilution refrigerator at our disposal we built a new dilution refrigerator with a maximum circulation rate of 2.5 mmol/s. The main topics of this machine are described in chapter V.

The theory of the double and triple mixing chamber will be described extensively in chapter VI.

Measurements concerning the DMC will be given in chapter VII.

In this thesis SI units are used, unless otherwise stated.

References.

- Coops, G.M., Waele, A.Th.A.M. de and Gijsman, H.M., *Cryogenics* 19 (1979) 659.
- Das, P., Bruyn Ouboter, R. de, Taconis, K.W., Proc. LT 9, Columbus, Ohio (1964), (Plenum Press, New York, 1965) 1253.
- Edwards, D.O., Brewer, D.F., Seligman, P., Skertic, H. and Yagub, M., *Phys. Rev. Lett.* 15 (1965) 773.
- Frossati, G., Schumacher, G., Thoulouze, D., Proc. LT 14 North Holland/American Elsevier (1975) 13.
- Frossati, G., Godfrin, H., Hébral, B., Schumacher, G., Thoulouze, D., Proc. Hakone, Int. Symp., Japan (1977) ed. T. Sugawara, Phys. Soc. of Japan.
- Haeringen, W. van, *Cryogenics* 20 (1980) 153.
- Haeringen, W. van, Staas, F.A. and Geurst, J.A., *Philips Journal of Research* 34 (1979) 107.
- Haeringen, W. van, Staas, F.A. and Geurst, J.A., *Philips Journal of Research* 34 (1979) 127.
- Hall, H.E., Ford, P.J., Thompson, K., *Cryogenics* 6 (1966) 80.
- London, H., Proc. Int. Conf. Low Temp. Phys., Oxford (Clarendon Lab, 1951) 157.
- London, H., Clarke, G.R., Mendoza, E., *Phys. Rev.* 128 (1962) 1992.
- Neganov, B.S., *Vestn. Akad. Nauk. S.S.S.R.* no. 12 (1968) 49.
- Niinikoski, T.O., *Nucl. Instr. Meth.* 97 (1971) 95.
- Radebaugh, R., (1967) U.S. N.B.S. Techn. Note no. 362.
- Siegwarth, J.D., Radebaugh, R., *Rev. Sci. Instr.* 43 (1972) 197.
- Staas, F.A., Weiss, K., Severijns, A.P., *Cryogenics* 14 (1974) 253.
- Staas, F.A., Severijns, A.P., Waerden, H.C.M. van der, *Phys. Lett.* 53A (1975) 327.
- Taconis, K.W., Pennings, N.H., Das, P. and Bruyn Ouboter, R. de, *Physica* 56 (1971) 168.
- Taconis, K.W. *Cryogenics* 18 (1978) 459.
- Waele, A.Th.A.M. de, Reekers, A.B., Gijsman, H.M., *Physica* 81B (1976) 323.
- Waele, A.Th.A.M. de, Reekers, A.B., Gijsman, H.M., Proc. 2nd Int. Symp. on Quantum Fluids and Solids, Sanibel Island, Fla, USA (1977) ed. Trickey, Adams, Dufty, Plenum Publ. Cy (1977) 451.
- Walters, G.K., Fairbanks, W.M., *Phys. Rev.* 103 (1956) 262.

- Wheatley, J.C., Vilches, O.E. and Abel, W.R., Physics 4 (1968) 1.
- Wheatley, J.C., Rapp, R.E. and Johnson, R.T., J. Low Temp. Phys. 4 (1971) 1.

THE PRINCIPLES OF DILUTION REFRIGERATION.2.1 Introduction.

In this chapter we will give a general description of a dilution refrigerator and summarize the important parameters and physical quantities which are necessary in the following chapters. We will only deal with the ^3He circulating machines.

Many papers have been written on this subject, see for instance Wheatley (1968, 1971) and Radebaugh and Siegwarth (1971). Lounasmaa (1974) and Betts (1976) give reviews in their books. However, much progress has been made since 1976; the most recent summary is given by Frossati (1978).

2.2 The ^3He circulating dilution refrigerator.

In fig. 2.1 the phase diagram of ^3He - ^4He mixtures at saturated vapour pressure is presented. The phase separation was discovered

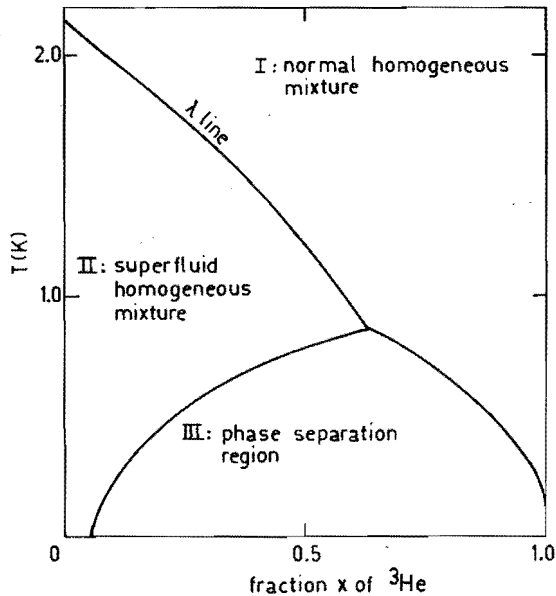


Fig. 2.1 The phase diagram of liquid ^3He - ^4He mixtures at saturated vapour pressure.

by Walters and Fairbank (1956). De Bruyn Ouboter et al. (1960), Brewer and Keyston (1962) and Edwards et al. (1965) investigated this diagram extensively. It turned out that the diagram consists of three regions. In the first region both components are normal. In the second region the ^4He in the mixture is superfluid. If a combination of temperature and composition corresponding to a point in region III is chosen, a phase separation will occur: a phase with a high concentration of ^3He (the concentrated phase) and a phase with a low concentration of ^3He (the diluted phase) can exist in equilibrium. The concentrated phase has a lower density and will be floating on top of the dilute phase. In fig. 2.1 we also see that even at the lowest temperatures it is possible to dissolve ^3He into ^4He up to a concentration of 6.4%. The flow diagram of a dilution refrigerator is given in fig. 2.2. In order to condense the ^3He two flow impedances are necessary: one below the 1 K plate and one below the still. They provide a ^3He pressure higher than the local condensation pressure of ^3He . Usually the ^3He gas is condensed at a pressure of about 13 kPa (100 torr) on the 1 K plate.

In fig. 2.3 the enthalpy-pressure (H-p) diagram of ^3He is presented (Roubeau, private communication). With the aid of this diagram we will explain why it is important to choose correct values of these impedances. In the first or main impedance the ^3He is throttled to lower pressures and a fraction of vapour is formed. A second impedance provides a sufficiently high pressure to establish the condensation of this vapour by extracting heat through the still heat exchanger.

If this impedance is chosen incorrectly the ^3He liquid, formed in the 1 K plate, will vaporize in the still heat exchanger leading to malfunctioning of the machine. Below the secondary impedance the pressure is determined by the flow resistances and the hydrostatic pressure, which is enough to prevent boiling of the ^3He .

The liquid ^3He exchanges heat with the cold dilute stream, coming from the mixing chamber. Finally it enters the mixing chamber, where by crossing the phase boundary the dilution takes place. In the dilute phase the ^3He flows back to the still. It is important that the flow resistance along this path is small, as

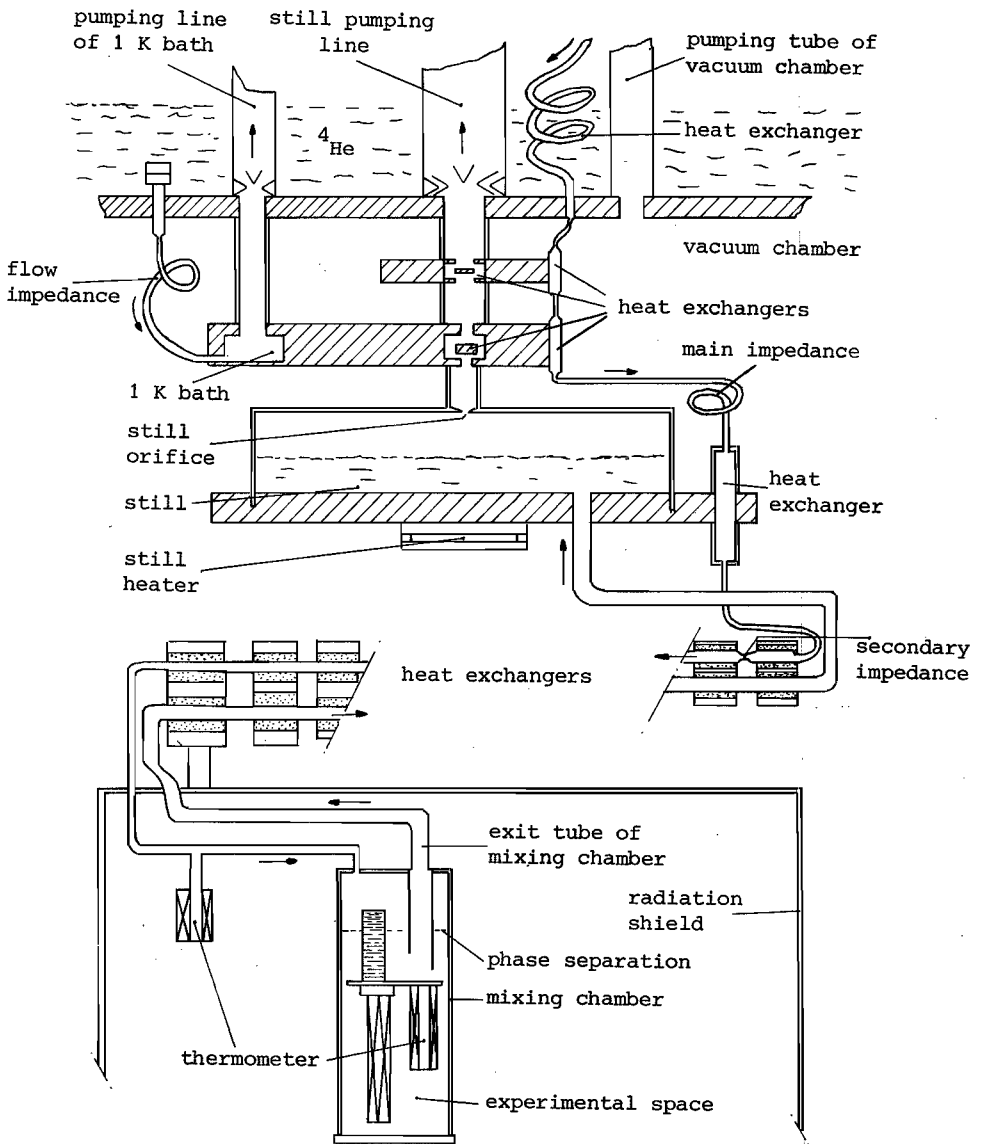


Fig. 2.2 Schematic diagram of a dilution refrigerator.

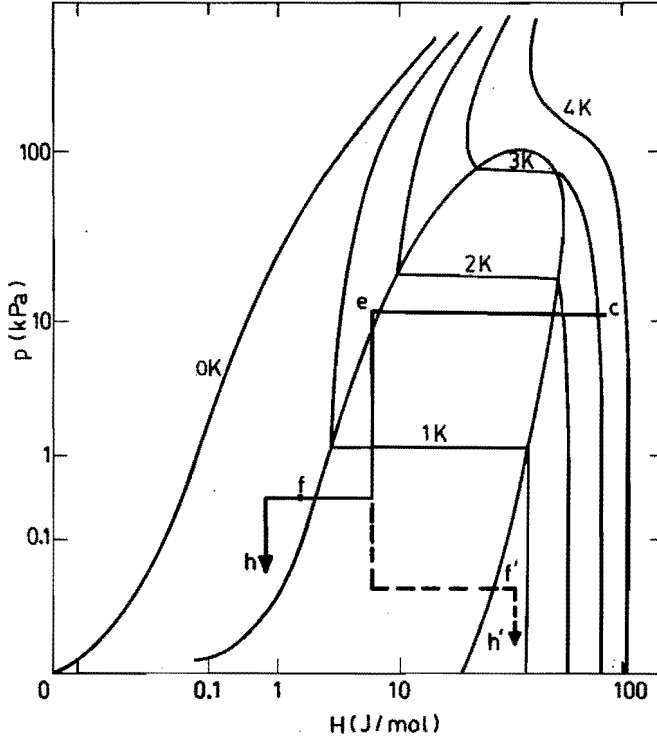


Fig. 2.3 The pressure vs. enthalpy curves of ^3He . The curve cefh presents the way the impedances are chosen for normal functioning of the dilution refrigerator. The curve cef'h' leads to a malfunctioning of the machine. The letters in this figure correspond to the set-up described in fig. 5.4.

can be seen as follows (for convenience the hydrostatic pressure is neglected). In the stationary state both ^3He and ^4He must obey an equation of motion with $\partial v/\partial t = 0$. From this requirement it follows that the gradient of the chemical potential of the ^4He is zero ($\nabla\mu_4 = -m_4\partial v_s/\partial t = 0$). Therefore the difference $p - \Pi$ between pressure and osmotic pressure is constant in the dilute phase (Lounasmaa, 1974) if the fountain pressure can be neglected (as is the case below 0.7 K). As a consequence

$$p_s - \Pi_s = p_m - \Pi_m, \quad (2.1)$$

where p_s and Π_s are the pressure and osmotic pressure in the still and p_m and Π_m the pressure and osmotic pressure in the mixing chamber respectively. The pressure differences in the system are caused by ^3He which is circulated by the external pumps. The pressure in the still is $p_s \approx 0$. For a flow resistance Z_d at the dilute side and a ^3He flow \dot{n}_3 , the pressure in the mixing chamber is given by $p_m = \dot{n}_3 Z_d V_d \eta$, so eq. (2.1) can be written as:

$$\Pi_s = \Pi_m - \dot{n}_3 Z_d V_d \eta, \quad (2.2)$$

with V_d the molar volume and η the viscosity of diluted ^3He . Hence a flow resistance in the dilute side at a given flow rate causes a pressure in the mixing chamber, whereas the osmotic pressure Π_m has the value of 12 torr. According to that, the osmotic pressure in the still decreases, leading to a reduction of the ^3He concentration in the still. This leads to a decrease in the partial vapour pressure of the ^3He in the still. If the pressure in the mixing chamber would be 12 torr, the ^3He concentration in the still would be zero and the dilution refrigerator fails to operate properly. The flow channels at the dilute side will be chosen in such a way that this effect cannot occur.

Vapour is removed from the still by pumping. More than 95% of the outcoming gas is ^3He because the partial vapour pressure of ^4He is much smaller than of ^3He in the still below 0.7 K. In this way the ^3He is separated from the ^4He . Finally the ^3He is pressurized again by pumps at room temperature.

In this thesis the influence of the small fraction ^4He that is circulated with the ^3He will be neglected.

2.3 Enthalpy considerations.

The ^3He isotope has a (nuclear) spin 1/2. Although the interactions between the atoms are rather strong, Fermi statistics can be applied if the ^3He mass (m_3) is replaced by an effective mass m_3^* . The specific heat per mole well below the Fermi temperature ($T \ll T_F$) is then given by:

$$C_v = \frac{m_3^* k^2 N_A}{\hbar^2} \left(\frac{\pi}{3} \frac{V_m}{N_A} \right)^{2/3} T. \quad (2.3)$$

In this formula k is the Boltzmann constant, N_A is Avogadro's number, \hbar is Planck's constant and V_m is the volume of one mole of ^3He . The specific heat in the concentrated phase has been measured by several authors (Anderson, 1966b; Abel, 1966) and can be represented by eq. (2.3) with $m_3^* \approx 2.8 m_3$ and $V_m = 37 \times 10^{-6} \text{ m}^3 \text{ mol}^{-1}$.

$$C_{3c} = 24 T \quad (2.4)$$

and thus for the entropy per mole:

$$S_{3c} = 24 T \quad (2.5)$$

and for the enthalpy, with $H_{3c}(0) = 0$:

$$H_{3c} = 12 T^2. \quad (2.6)$$

The specific heat of the dilute phase with $x = 6.4\%$ is given with sufficient accuracy by that of a Fermi gas, the density of which is the same as the density of the ^3He in the dilute solution (Anderson, 1966a, 1966b; Radebaugh, 1967); formula (2.3) then gives with $m_3^* \approx 2.5 m_3$ and $V_m = V_d = 430 \times 10^{-6} \text{ m}^3 \text{ mol}^{-1}$

$$C_{3d} = 108 T. \quad (2.7)$$

We obtain for the entropy in the dilute solution:

$$S_{3d} = 108 T. \quad (2.8)$$

In equilibrium the chemical potentials μ_{3c} and μ_{3d} in the concentrated and the diluted phase are equal:

$$\mu_{3c} \equiv H_{3c} - TS_{3c} = H_{3d} - TS_{3d} \equiv \mu_{3d}. \quad (2.9)$$

With eqs. (2.5), (2.6) and (2.8) we find for the enthalpy in the dilute phase along the saturation curve:

$$H_{3d} = 96 T^2 . \quad (2.10)$$

For the enthalpy of dilute ^3He at constant osmotic pressure Π (for instance in the heat exchangers) we find:

$$H_{\pi} = 54 T^2 + 42 T_m^2 \quad (2.11)$$

which is based on the eqs. (2.7) and (2.10). In this equation T_m is the temperature of the mixing chamber.

With the eqs. (2.6) and (2.10) one obtains the heat balance of the mixing chamber:

$$\dot{Q}_m = \dot{n}_3 (96 T_m^2 - 12 T_i^2) , \quad (2.12)$$

where T_i is the temperature of the incoming ^3He , \dot{Q}_m is the total heat load and \dot{n}_3 is the ^3He flow rate.

When there is no heat leak and no external heating eq. (2.12) simplifies to:

$$T_m = 0.36 T_i . \quad (2.13)$$

From these equations we see that it is necessary to precool the ^3He effectively. Moreover, the viscous heating and the heat conducted to the mixing chamber have to be minimized.

References.

- Abel, W.R., Anderson, A.C., Black, W.C., and Wheatley, J.C.,
Phys. Rev. 147 (1966) 111.
- Anderson, A.C., Roach, W.R., Sarwinski, R.E. and Wheatley, J.C.,
Phys. Rev. Lett. 16 (1966a) 263.
- Anderson, A.C., Edwards, D.O., Roach, W.R., Sarwinsky, R.E. and
Wheatley, J.C., Phys. Rev. Lett. 17 (1966b) 367.
- Betts, D.S., (1976) Refrigeration and Thermometry below 1 K,
Sussex Univ. Press.
- Brewer, D.F. and Keyston, J.R.G., Phys. Lett. 1 (1962) 5.
- Bruyn Ouboter, R. de, Taconis, K.W., Le Pair, C. and Beenakker, J.J.M.,
Physica 26 (1960) 853.
- Edwards, D.O., Brewer, D.F., Seligman, P., Skertic, M. and Yagub, M.
Phys. Rev. Lett. 15 (1965) 773.
- Frossati, G., Journal de Physique, Colloq. C6, suppl. 8, 39 (1978)
p. 1578.
- Lounasmaa, O.V., (1974) Experimental Principles and Methods below
1 K, Acad. Press, London.
- Radebaugh, R., (1967) U.S. N.B.S., Tech. Note, no. 362.
- Radebaugh, R. and Siegwarth, J.D., Cryogenics 11 (1971) 368.
- Roubreau, P., private communication.
- Walters, G.K., Fairbank, W.M., Phys. Rev. 103 (1956) 262.
- Wheatley, J.C., Rapp, R.E. and Johnson, R.T., J. Low Temp. Phys.
4 (1971) 1.
- Wheatley, J.C., Vilches, O.E. and Abel, W.R., Physics 4 (1968) 1.

CHAPTER III.

THERMOMETRY.

3.1 Introduction.

For temperatures below 1 K three types of thermometers have been used: magnetic thermometers with CMN, carbon resistance thermometers and NMR-thermometers with Pt powder. For the calibration of these, two NBS fixed point devices were used.

CMN thermometers can be used below 1 K. This technique is based on the temperature dependence of the magnetic susceptibility of powdered CMN, which has an almost perfect Curie behaviour down to 3 mK when special precautions are taken (see 3.3).

Devices with a temperature-dependent electrical resistance, such as carbon resistors, are the most commonly used thermometers at cryogenic temperatures down to 10 mK. The combination of small dimensions, ready availability and relative ease of measurement has resulted in their widespread application.

These thermometers were calibrated with two NBS fixed point devices, the first of which is based on the transition temperatures of Pb, Zn, Al, Sn and Cd, the second on the transition temperatures of AuIn₂, AuAl₂, Ir, Be, W (NBS, 1979).

Nuclear Magnetic Resonance (NMR) on platinum powder can also be used as a temperature standard down to about 2 mK. It is based on the measurement of the spin-lattice relaxation time of platinum. The product of this relaxation time and the temperature equals the Korringa constant which for platinum is equal to 30 mKs.

In this chapter we will deal with some aspects of resistance and CMN thermometry which have been investigated in our laboratory (Coops, 1980). (A review paper about these and other techniques is written by Hudson et al. (1975)).

3.2 Resistance thermometry and the maximum allowable dissipation.

Certain types of industrial carbon composition resistors are being used extensively as cryogenic temperature sensors at temperatures higher than 10 mK. Especially the Speer resistors are well-known. Resistance thermometers have a number of practical

advantages such as the ease of measurement and high relative sensitivity $\alpha = -(T/R) (dR/dT)$.

Joule heating in the resistor generated by the measuring current or by rf pick up has to be transferred to and across the surface of the thermometer and consequently its temperature in steady state is bound to be higher than the temperature to be measured. Oda et al. (1974) suggested a method to compare resistors and mounting methods. They measured a quantity P_m , which is the power supplied to the resistors for which its resistance falls by 1%. For the 220 Ω -type (Speer) they found

$$P_m \approx 2 \left(\frac{T}{K}\right)^{4.3} \mu W \quad 30 \text{ mK} < T < 1 \text{ K} , \quad (3.1)$$

and a slightly different value for the 100 Ω -type.

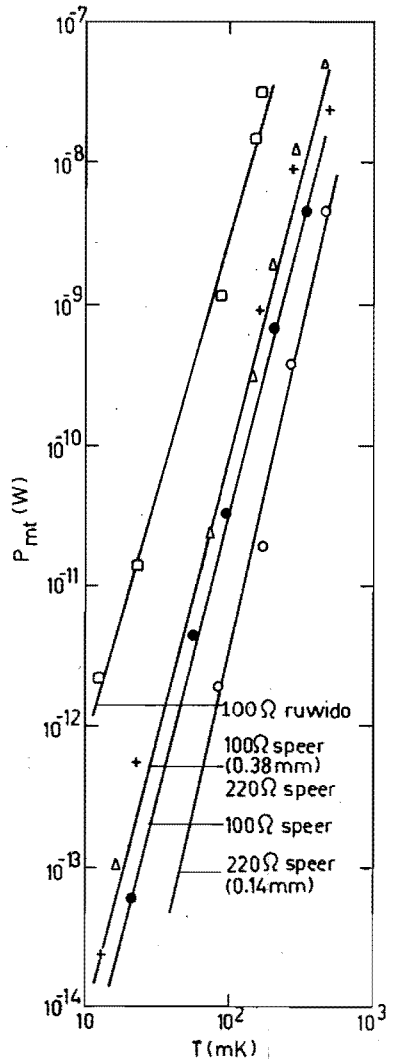
To compare resistors with different sensitivities it is useful to introduce a quantity P_{mt} , which is the power supplied to the resistor giving an effective temperature increase of 1%. The relation $P_{mt} = \alpha P_m$ holds and in a large temperature region α is a constant. We measured P_{mt} for several materials and several thicknesses. In fig. 3.1 P_{mt} vs. temperature is given for some typical resistive materials. The power relation can be written as:

$$P_{mt} = C T^\gamma . \quad (3.2)$$

In table 3.1 the constants C and γ are given for several resistive materials. We note that grinding of a resistor (e.g. 220 Ω Speer to a thickness of 0.14 mm and a 100 Ω Speer to 0.38 mm) does not increase the P_{mt} value significantly in all circumstances. The differences between the samples are not understood well at the moment, however, a $P_{mt} - T$ relation deduced from the heat balance inside the resistive material gives a calculated γ value which is in a good order of magnitude ($3 < \gamma < 5$). The values of Oda et al. (1974) and our values agree rather well at 30 mK. However, the 100 Ω resistor of Oda is able to dissipate 6x more than our resistor at this temperature. This difference could be due to differences between individual specimens. Such differences have also been noticed by Severijns (private communication). The behaviour of the resistors is according to Oda intrinsic

to the material. Other authors find relations which give similar results at low temperatures, (Anderson, 1971). If one wants to keep the level within the limit of eq. (3.2) the use of suitable instrumentation and mounting techniques is necessary. The measurements of this work were done with a Wheatstone-bridge, using a PAR124A lock-in amplifier as a null detector.

Fig. 3.1 The power supplied to the resistor giving an effective temperature increase of 1% vs. temperature. The resistors were mounted inside the mixing chamber.



3.3 CMN thermometry.

Cerous Magnesium Nitrate ($Ce_2Mg_3(NO_3)_{12} \cdot 24H_2O$) or CMN is used as a thermometer because the deviations from the Curie law are small down to a few mK. In most cases when CMN is used as a thermometer, it is powdered and pressed in the shape of a cylinder with the length equal to the diameter. In this configuration the deviation from the Curie law is the smallest at low temperatures (Webb et al., 1978). The relaxation time with a mixture of ^3He and ^4He becomes

Resistance Type	$\frac{P}{W} = C \left(\frac{T}{K}\right)^\gamma$		$P_{mt} \times 10^{12}$ at 30 mK	$\left(\frac{R}{k\Omega}\right) \approx B \left(\frac{T}{K}\right)^{-\alpha} \quad T < 0.1 \text{ K}$	
	$C \times 10^6$	γ		B	α
Speer 220 Ω 0.14 mm	0.03	3.8	0.05	0.32	2
Speer 220 Ω	1	3.7	2	0.21	1.7
Speer 220 Ω^*	3.4	4.3	1	0.13	1.7
Speer 100 Ω 0.38 mm	2	4.3	0.6	0.63	1.1
Speer 100 Ω^*	0.07	2.9	3	1.0	1.0
Speer 100 Ω	0.4	3.9	0.5	0.20	0.9
Speer 77 Ω (baked from 220 Ω)	1	4.1	0.6	0.17	0.94
Speer 47 Ω	3	3.2	4	0.08	0.7
Bourns 2 k Ω Type 4115R	0.01	2.7	0.8	3.8	0.64
Ruwido 1 k Ω Type 0042-320	300	4.6	3	1.3	0.25
Philips Cermet	0.1	2.9	4	3.2	0.2
Ruwido 100 Ω Type 0042-320	20	3.7	50	0.59	0.21
Amphenol 500 Ω Type 3805 P	3	3.3	30	0.92	0.1
Bourns 220 Ω Type 4114R	3	3.6	10	155	0.04

*Deduced from Oda (1974).

Table 3.1 The P_{mt} vs. T and R vs. T relations for several resistive materials and configurations.

rather large at low temperatures and is also dependent on the grain size (Chapellier, 1978).

In fig. 3.2 the configuration of our CMN thermometer is given. The CMN is pressed in an epibond or araldite holder to reduce thermal contact with the walls of the mixing chamber. The particle

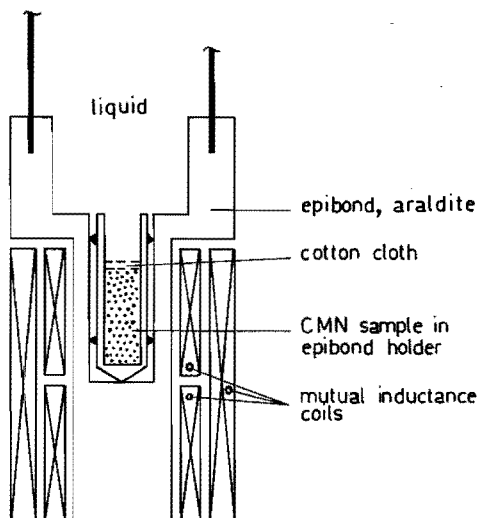


Fig. 3.2 The configuration of the CMN thermometer.

size of the powder varies between 1 and 20 μm ; the packing is about 80%. The susceptibility is measured by the mutual inductance coils in combination with a PARI24A lock-in amplifier. The CMN thermometers were calibrated against a NBS device directly and indirectly (via a Speer resistor) against a platinum NMR thermometer. These calibrations determined the constants A_0 and M_∞ in the relation $\Delta M = M - M_\infty = A_0/T$.

3.4 Thermometry with partly dehydrated CMN.

CMN dehydrates when it is pumped at room temperature (Butterworth et al., 1973). Butterworth et al. (1974) reported an increase of the Curie constant with a factor 2, when 16 of the initial 24 waters per formula unit are removed. They also suggested that the contraction of the crystalline structure would lead to a

larger interaction between the magnetic moments and hence to a higher ordering temperature.

With the aid of a calibrated Speer resistance the ΔM -T dependence of the CMN sample before and after dehydration was measured. The CMN was dehydrated by pumping at room temperature for about 250 hours. The result is shown in fig. 3.3. Below about 150 mK

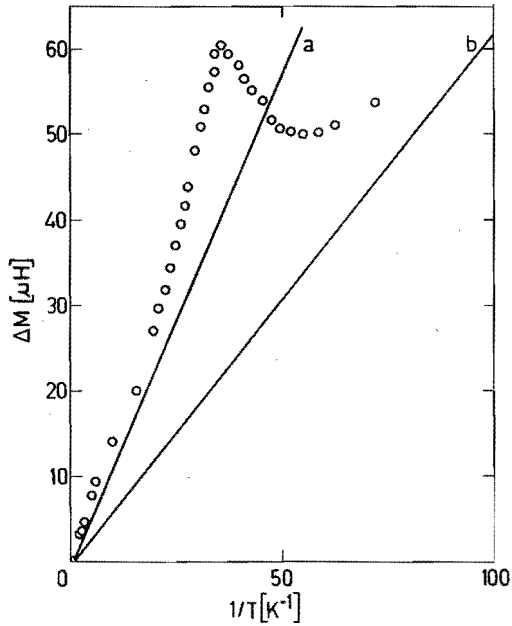


Fig. 3.3. Measured ΔM vs $1/T$ dependence for partly-dehydrated CMN. Also drawn in the figure are:
line a representing the calibration line for the non-dehydrated sample,
line b representing the Curie-Weiss behaviour of the 54% non-dehydrated CMN in the partly-dehydrated sample.

we observed a deviation from the Curie law. At 29 mK a maximum appears. This ΔM -T dependence can be qualitatively understood assuming that the CMN powder is effectively divided into a portion x that is completely dehydrated and a portion $(1-x)$ which is not dehydrated. This can be shown as follows. From the measured ΔM -T dependence one can derive $A' = \Delta M \cdot T$. The value

of A' is temperature dependent. In the high temperature region $A' = 1.46 A_0$. As for completely dehydrated CMN the A value equals $2 A_0$ (Butterworth et al., 1974) we calculated from our experiment $x = 0.46$. According to our model the remaining 54% CMN is not dehydrated and will follow a Curie law as usual. It gives a contribution to A' equal to $0.54 A_0$. This contribution will dominate the contribution of the dehydrated part at low temperatures. In our dilution refrigerator with a double mixing chamber (Coops et al., 1979) we determined the ΔM values for the lowest temperatures in the continuous and single cycle mode. With $\Delta M = 0.54 A_0 / T$ (line b) these temperatures were in good agreement with the limiting temperatures normally reached. After these experiments, the CMN was exposed to air at room temperature and the increase in weight due to absorption of water was measured. From this measurement it was calculated that 47% of the CMN was effectively dehydrated, which is in good agreement with the 46% we found above. These experiments make clear that partly dehydrated CMN does not follow a Curie law in the whole temperature region. When nevertheless a Curie law is assumed an apparent temperature T_a is measured, different from the real temperature T . For a given value of x it is possible to calculate the real temperature from the apparent temperature T_a . We distinguish two experimental procedures. The first is that a calibration is done of a non-dehydrated CMN thermometer ($x = 0$), which is assumed to be unchanged for the rest of the experiments even after pumping the thermometer at room temperature. In this case the relations between T_a and T are the following

$$T_a = T(1 + x)^{-1} \quad T \geq 150 \text{ mK} \quad 0 < x < 1 \quad (3.3)$$

and

$$T_a = T(1 - x)^{-1} \quad T \ll 29 \text{ mK} \quad 0 < x < 1 \quad (3.4)$$

In the second case a calibration of the partly dehydrated CMN thermometer is done between 0.5 K and 4.2 K before every experiment. Here T_a follows from this calibration, assuming

(erroneously) a Curie behaviour at low temperatures. We then find for the relation between T_a and T

$$T_a = T \quad T \gg 150 \text{ mK} \quad (3.5)$$

and

$$T_a = T(1 + x)(1 - x)^{-1} \quad T \ll 29 \text{ mK} \quad (3.6)$$

These experiments show that good care has to be taken with measurements and calibrations with CMN thermometers, especially when one has to pump the systems with the thermometers inside. Even a calibration of a pumped CMN thermometer does not guarantee correct temperature measurements in the low temperature region.

3.5 Dehydration and saturated vapour pressure of CMN.

As has been shown, it is important that CMN in a thermometer is not dehydrated. The vapour pressure of partially dehydrated CMN is measured by Butterworth and Bertinat (1973). They found (fig. 3.4):

$$\log p = 10.05 - 3.06 \times 10^3/T \quad (3.7)$$

where p is in torr and T in Kelvin. We verified this formula at two temperatures: room-temperature (21°C) and 64°C and we found an excellent agreement with eq. (3.7). These measurements show that it is advisable not to pump CMN and to maintain the relative humidity above 2.4% at room-temperature.

However, it is also important that the grain size of the powdered CMN is small, this with respect to the time constants which become important at low temperatures (Chapellier, 1978). CMN is a little hygroscopic and with a high humidity it will liquefy, when the humidity is lowered afterwards recrystallization will occur. After recrystallization larger crystals are formed, which will give higher time constants for the CMN thermometer at low temperatures. For this reason it is advisable to have a vapour pressure below the saturated vapour pressure of CMN for which we found (Reints, 1980) (fig. 3.4):

$$\log p = 7.95 - 2.01 \times 10^3/T \quad (3.8)$$

where p in torr and T in Kelvin.

From this formula and the vapour pressure of water we find that at 20°C and a relative humidity of 73% liquefying will occur. The difference in slope between the curve of water and saturated CMN is caused by the heat of solution of CMN in water.

These measurements show that it is advisable to store CMN and CMN thermometers for values of p and T between curves a and b in fig. 3.4 in order to avoid dehydration and recrystallization after liquefying.

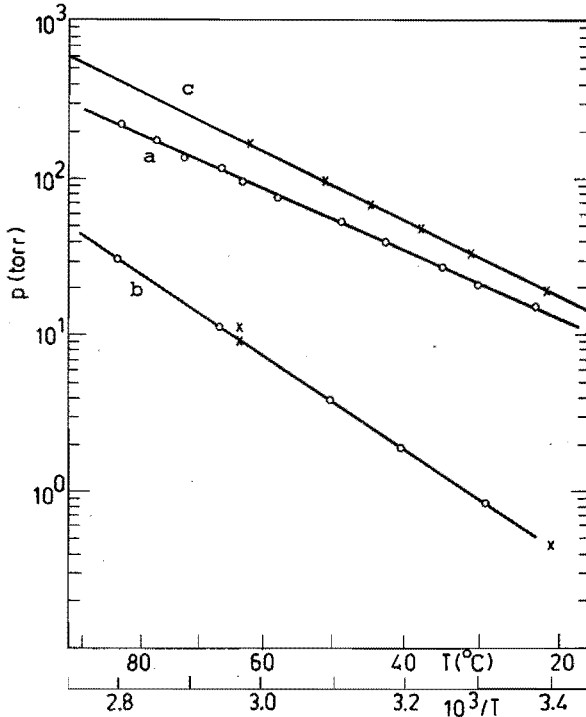


Fig. 3.4 The vapour pressures of water and CMN.
 Line a: saturated solution of CMN.
 Line b: dry CMN.
 Line c: water.

References.

- Anderson, A.C., Temperature: Its Measurement and Control in Science and Industry, vol. 4 (ed. H.H. Plumb, Instrument Society of America, 1972) part 2, p. 773.
- Butterworth, G.J. and Bertinat, M.P., Cryogenics, vol. 13 (1973) p. 282.
- Butterworth, G.J., Finn, C.B.P. and Kiyamac, K., J. Low Temp. Phys., 15 (1974) 537.
- Chapellier, M., Proc. of the 15th LT conf., Journal de Physique (Paris), Colloq. C-6, suppl. 8 (1978) p. 273.
- Coops, G.M., Waele, A.Th.A.M. de and Gijsman, H.M., Cryogenics 19 (1979) 659.
- Coops, G.M. Reekers, A.B., Waele, A.Th.A.M. de, Gijsman, H.M., Proc. ICEC 8, IPC Science and Technology Press (1980) 731.
- NBS, Special Publication 260-2 (1979).
- Oda, Y., Fujii, G. and Nagano, H., Cryogenics 14 (1974) 84.
- Reints, H., Internal report 1980.
- Severijns, A.P., private communication.
- Webb, R.A., Griffard, R.P. and Wheatley, J.C., J. Low Temp. Phys., 13 (1978) 383.

CHAPTER IV.

THE DESIGN OF TUBES AND HEAT EXCHANGERS AND THE CONSEQUENCE ON THE MINIMUM TEMPERATURE OF A DILUTION REFRIGERATOR.

4.1 Introduction.

The lowest temperature that can be obtained with a dilution refrigerator has always been an important point of discussion. Wheatley (1968) pointed out that the minimum temperature depends on the combined effects of cooling power, viscous heating and heat conduction and therefore on the sizes of the tubes to and from the mixing chamber.

Heat exchangers were also investigated and in 1971 Niinikoski introduced a heat exchanger with an open channel through the sinter sponge to lower the viscous heating. Extending this concept and the work of Siegwarth (1972) and Staas (1974), Frossati (1977) succeeded in lowering the temperature of the mixing chamber to 2 mK by means of heat exchangers using silver as the sinter material.

In this chapter we will not deal with the methods avoiding the Kapitza resistance, such as ^4He circulating machines and multiple mixing chambers.

4.2 Design considerations concerning tubes.

Wheatley (1968) showed that in order to calculate the influence of heat conduction and viscous heating on the performance of the mixing chamber, one has to solve a differential equation derived from the heat balance in a tube. For the dilute side he derived:

$$3.8 \times 10^{-13} \frac{\dot{n}_3^2}{T_d^2 d_d^4} + 2.4 \times 10^{-4} d_d^2 \frac{d}{d\ell} \left(\frac{1}{T} \frac{dT}{d\ell} \right) = 108 \dot{n}_3 T \frac{dT}{d\ell} \quad (4.1)$$

where \dot{n}_3 is the ^3He flow rate, ℓ the position in the tube and d_d the diameter. The first term on the left hand side of eq. (4.1) is due to viscous heating, the second term to heat conduction and the right hand term to enthalpy flow. From this equation one can introduce a characteristic temperature T_d^* :

$$T_d^* = 4.4 \times 10^{-4} d_d^{-1/3} \quad (4.2)$$

and a characteristic length l_d^* :

$$l_d^* = 11 d_d^{8/3} \dot{n}_3^{-1} \quad (4.3)$$

where d_d is the diameter of the tube.

The characteristic volume of the tubes in a dilution refrigerator is, as can be seen from eqs. (4.2) and (4.3), inversely proportional to $\dot{n}_3 T^{14}$. This shows that for lower temperatures larger machines will be necessary both with respect to volume and circulation rate. The heat balance eq. (4.1) and a similar one for the concentrated side can be solved exactly as has been shown by Van Haeringen (1979a, 1979b, 1980). For an order-of-magnitude calculation, which is often sufficient, we assume that for the dilute side:

- the conducted heat is independent of the ^3He flow \dot{n}_3 and equal to $\dot{Q}_c = \frac{\pi d_d^2}{4 l_d} \kappa_d \ln \frac{T_i}{T_o}$.
- Viscous heating is estimated by $\dot{Q}_v = Z_d \frac{\eta_d}{T^2} \dot{n}_3^2 V_d^2$ where Z_d is the impedance of the tube and V_d the molar volume of ^3He and T a typical temperature of the liquid in the tube.
- The enthalpy flow is given by $\dot{H} = c \dot{n}_3 T^2$ where c is constant and T an average temperature of the liquid in the tube.

For a good design we require that $\dot{Q}_v, \dot{Q}_c \ll \dot{H}$ and similar restrictions for the concentrated side.

This calculation leads to a similar result as the exact solution and will be given below.

4.2.1 The concentrated side.

The condition that the viscous heating rate is much smaller than the enthalpy flow, for temperatures below 40 mK, at the concentrated side leads to:

$$Z_c \frac{\eta_c}{T^2} \dot{n}_3^2 V_c^2 \ll 12 \dot{n}_3 T^2. \quad (4.4)$$

T is a typical temperature of the liquid, Z_c is the flow impedance of the tube, η_c/T^2 is the viscosity and V_c is the molar volume of pure ^3He . The condition that the heat flow due to conduction is small compared to the enthalpy flow leads to:

$$\frac{\pi d_c^2}{4l_c} \kappa_c \ln \frac{T_{ci}}{T_{co}} \approx \frac{\pi d_c^2}{4l_c} \kappa_c \ll 12 \dot{n}_3 T^2 . \quad (4.5)$$

Here κ_c/T is the heat conduction and l_c and d_c are the length and the diameter of the tube respectively. In this inequality we assumed that the ratio between the temperatures at the two ends of the tube is two, which is generally true. In this case we give a pessimistic estimation of the conducted heat, because we neglected the influence of the flow. For a tube with a diameter d_c and an impedance for laminar flow $Z_c = 128 l_c / \pi d_c^4$, the conditions (4.4) and (4.5) can be combined to:

$$\frac{\pi d_c^2 \kappa_c}{48 \dot{n}_3 T^2} \ll l_c \ll \frac{12 \pi T^4 d_c^4}{128 \eta_c \dot{n}_3 V_c^2} . \quad (4.6)$$

From (4.6) the following numerical result can be derived taking $\eta_c = 2 \times 10^{-7} \text{ PaK}^4 \text{ s}$ (Betts, 1972) and $\kappa_c = 3.6 \times 10^{-4} \text{ W m}^{-1}$ (Wheatley, 1968):

$$2.4 \times 10^{-5} \frac{d_c^2}{\dot{n}_3 T^2} \ll l_c \ll 10^{15} \frac{T^4 d_c^4}{\dot{n}_3} . \quad (4.7)$$

A value for l_c satisfying (4.7) can only be found when:

$$T \gg 5.4 \times 10^{-4} d_c^{-1/3} . \quad (4.8)$$

4.2.2 The dilute side.

For the dilute side one can similarly derive for temperatures below 20 mK, with $\eta_d = 0.5 \times 10^{-7} \text{ PaK}^4 \text{ s}$ and $\kappa_c = 3.0 \times 10^{-4} \text{ Wm}^{-1}$:

$$4.4 \times 10^{-6} \frac{d_d^2}{\dot{n}_3 T^2} \ll l_d \ll 1.5 \times 10^{15} \frac{T^4 d_d^4}{\dot{n}_3} \quad (4.9)$$

which can only be satisfied if:

$$T \gg 5.5 \times 10^{-4} d_d^{-1/3} = 1.3 T_d^x . \quad (4.10)$$

Although the constants in the conditions (4.8) and (4.10) are nearly equal, the dimensions of the tubes of the dilute side must be larger, because of the lower temperatures. The values of

Wheatley (1968), Frossati (1978) and Van Haeringen (1979a, 1979b, 1980) are in agreement with eq. (4.9). The results of Wheatley can be used to calculate the temperature of the mixing chamber T_m as a function of the temperature of the incoming ^3He for different values of the diameter of the exit tube (De Waele, 1976) (fig. 4.1).

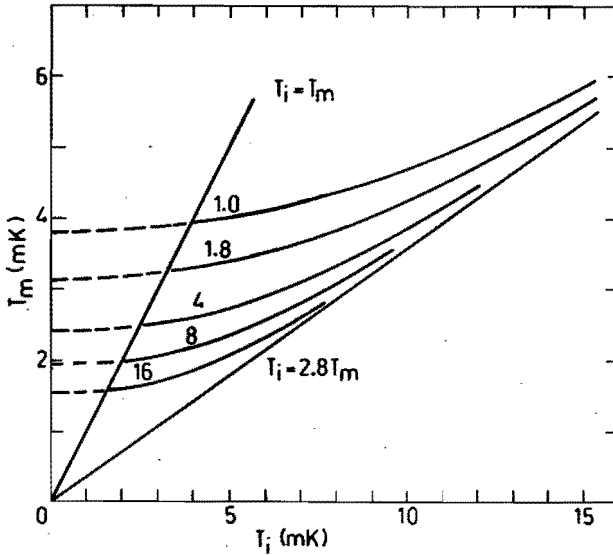


Fig. 4.1 Dependences of the single mixing chamber temperature T_m on the temperature T_i of the incoming ^3He when viscous heating is taken into account. Curves are drawn for 5 different diameters of the exit tube ($d = 1.0, 1.8, 4.0, 8.0$ and 16 mm). The intersection points of the curves with the line representing $T_i = T_m$ give the limiting values of T_m in the single cycle mode. The line marked $T_i = 2.8 T_m$ represents the $T_i - T_m$ dependence when viscous heating is neglected ($d \rightarrow \infty$). In the region in which $T_i < T_m$ the curves are drawn with broken lines.

4.3 Design considerations for heat exchangers.

Continuous counterflow heat exchangers, in which the temperature of the heat exchanger body changes continuously with distance and step heat exchangers in which the body temperature is practically constant are used since many years. The continuous heat exchanger is economic in size and helium content, whereas the sintered step

heat exchanger is less efficient. A perfect step heat exchanger of which the temperature of the liquids leaving the heat exchanger are equal, gives a temperature reduction of about 50%. The efficiency of the exchange surface is low, because a large surface is necessary to equalize the temperature of the liquids and the wall. For reasons of construction we choose an intermediate form.

In our machine we use a semi-continuous heat exchanger. This is an exchanger consisting of a large number of step heat exchangers each giving a temperature reduction smaller than 50%. In our case it is 25%, thus avoiding ineffective heat exchange between the liquid and the body. From the heat balance of the mixing chamber it follows that for a given flow rate the minimum temperature of a dilution unit is determined by the temperature T_i of the concentrated ^3He entering the mixing chamber and the heat load on the mixing chamber. The value of T_i is a function of the total surface area σ of the heat exchanger. We give here a derivation of this function for the case of a continuous heat exchanger (fig. 4.2).

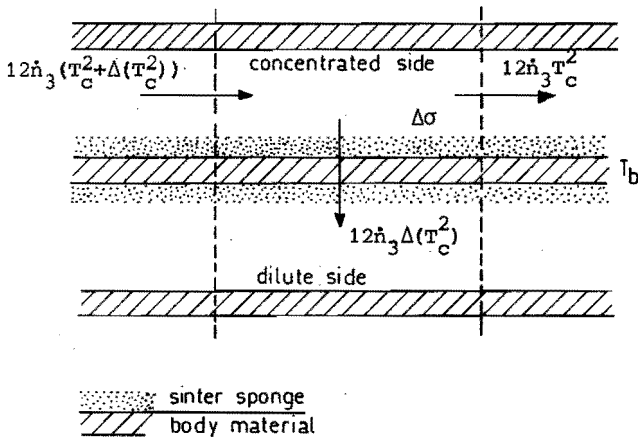


Fig. 4.2 Enthalpy balance and temperatures in a section of an ideal continuous heat exchanger.

The difference in enthalpy $\Delta \dot{H}_c$ along a small section of the heat exchanger at the concentrated side:

$$\Delta \dot{H}_c = 12 \dot{n}_3 \Delta(T_c^2) \quad (4.11)$$

is equal to the heat transported to the diluted side, which is determined by the Kapitza resistance and the temperature differences between the liquids and the body:

$$\dot{\Delta H}_c = \frac{\Delta\sigma_c}{4R_{Kc}} (T_c^4 - T_b^4) = \frac{\Delta\sigma_d}{4R_{Kd}} (T_b^4 - T_d^4) . \quad (4.12)$$

For a continuous heat exchanger with equal surfaces and equal Kapitza coefficients on the concentrated and the dilute side and with $T_d^4 \ll T_c^4$ one finds from eq. (4.12) with $R_K = R_{Kd} = R_{Kc}$

$$\dot{\Delta H}_c = T_c^4 \Delta\sigma_c / 8R_K \quad (4.13)$$

and $T_b \approx 0.8 T_c$.

Integration now yields:

$$\sigma_c = 96 R_K \dot{n}_3 \left[\frac{1}{T_{co}^2} - \frac{1}{T_{ci}^2} \right] \approx \frac{96 R_K \dot{n}_3}{T_i^2} \quad (4.14)$$

with T_i the temperature of the ^3He entering the mixing chamber and $1/T_{co}^2 \gg 1/T_{ci}^2$.

The design features of heat exchangers have been discussed by many authors (Wheatley, 1968; Siegwarth, 1972; Staas, 1974; Niinikoski, 1976; Frossati, 1978 and others). A good continuous heat exchanger has to satisfy the following conditions:

I. The heat conducted in the liquid in the direction of the flow (or opposite to it) can be neglected compared to the heat exchanged.

II. The heat conducted by the heat exchanger body parallel to the flows can be neglected compared to the heat exchanged.

An exchanger satisfying these two conditions has a long and slender geometry. Viscous heating might become a problem. We therefore formulate a third condition:

III. Viscous heating must be small compared to the heat transported.

In order to have a good efficiency, there are two additional requirements.

IV. There must be sufficient surface area in the heat exchanger.

V. The thermal resistance of the sinter sponge and of the helium

in it perpendicular to the flow, must be sufficiently small compared to the Kapitza resistance.

Conditions similar to I and III apply to interconnecting tubes.

This subject has been treated in section 4.2.

We will now discuss the other conditions for a heat exchanger and use the following notation (fig. 4.3): S_b is the area of the cross

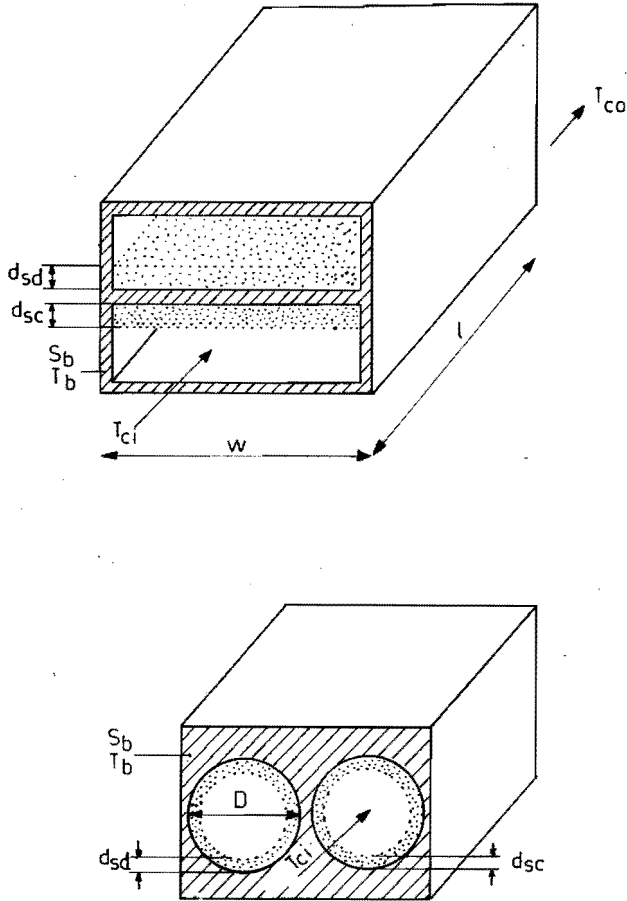


Fig. 4.3 The configuration of heat exchangers and the definition of the notations used in the test.

section of the body, l is the length of the heat exchanger, d_{sc} and d_{sd} are the thickness of the sinter sponge at the concentrated and dilute side respectively. The width of the exchanger channel is called w .

The liquid temperatures at the entrance and exit of the concentrated side are T_{ci} and T_{co} respectively. The body temperature is called T_b . The derivation also applies to a circular cross section. In that case w is π times the diameter of the hole.

Condition II leads to the following relation:

$$\frac{S_b}{2\ell} \kappa_b (T_{bi}^2 - T_{bo}^2) \ll 12 \dot{n}_3 (T_{ci}^2 - T_{co}^2) \quad (4.15)$$

with $\kappa_b T$ the thermal conductivity of the body material. From this equation and the fact that $T_b \approx 0.8 T_c$ one can derive:

$$\frac{S_b}{\ell} \ll \frac{48 \dot{n}_3}{\kappa_b} . \quad (4.16)$$

This equation shows that the cross-section S_b of the body is independent of the temperature, so all bodies can be constructed in the same way.

To satisfy condition IV we have to calculate the enthalpy difference between the entrance and the exit of the heat exchanger. If we have a heat exchanger which gives a temperature reduction from $2T_{co}$ to T_{co} this enthalpy difference is equal to:

$$\dot{q} = 12 \dot{n}_3 \{ (2T_{co})^2 - (T_{co})^2 \} = 36 \dot{n}_3 T_{co}^2 . \quad (4.17)$$

This is equal to the heat which is transported to the dilute side (compare eq. (4.13)).

With eq. (4.14) we get for the total surface area on the concentrated side σ_{ci} in the heat exchanger:

$$\sigma_{ci} = \frac{72 R_c \dot{n}_3}{T_{co}^2} . \quad (4.18)$$

Satisfying condition V ensures a good efficiency of the sinter material. The thickness of the sinter sponge with respect to the heat conduction in the helium and with respect to the heat conduction in the sinter sponge material are important.

The conductivity of copper is proportional to T and the conductivity of the helium liquid is proportional to T^{-1} . At higher temperatures the thermal conductivity of helium is smaller. The values meet in the mK region. In most cases ($T > 3$ mK) the thickness is

determined by the conductivity of the ^3He . We note that this conductivity decreases in small channels with diameter δ ($\kappa \approx \kappa_{\text{bulk}} \delta/\lambda$) and at very low temperatures (Betts, 1974), because the mean free path (λ) of the ^3He quasiparticles given by $\lambda = 3 \times 10^{-11} T^{-2}$ becomes equal to the channel diameter between the grains.

A similar effect occurs in the sinter material, where the heat conduction is caused by the electrons. A typical mean free path for electrons in reasonably pure (RRR ≈ 100) bulk noble metal at low temperatures is $5 \mu\text{m}$. Many sinters used for heat exchange are made from powders with diameters much smaller than $5 \mu\text{m}$. Then the electron mean free path will be boundary - rather than impurity - limited. Furthermore, the path for heat flow will contain many necks, pushing the resistance even further above the bulk value (Harrison, 1979).

In our last heat exchanger with a channel diameter between the grains of $\delta \approx 3 \mu\text{m}$ and a temperature of about 25 mK we are just at the border of this region. We will not take into account mean free path effects.

We will now, as an example, give the design considerations, with respect to condition V, in the low temperature limit

For the higher temperatures a numerical approach is advisable, although some of the conclusions given below also apply to the high temperature region.

Using again the dimensions introduced in fig. 4.3 and taking a filling factor for the copper $\nu = \rho_c/\rho_0$ with ρ_0 the density of the bulk material and ρ_c the density of the sinter sponge at the concentrated side, then the order of magnitude of the temperature differences, ΔT ($\ll T$), in the concentrated ^3He in the sinter is given by:

$$\dot{q} = \kappa_{\text{oc}} \frac{(1 - \nu) w \ell}{2d_{\text{sc}}} \frac{\Delta T_c}{T_c}, \quad (4.19)$$

in which $2d_{\text{sc}}$ is an estimation of the effective channel length of the ^3He channels. The heat \dot{q} , transported by the ^3He , is given by eq. (4.17) and in combination with eq. (4.19) we find:

$$d_{\text{sc}} = \frac{\kappa_{\text{oc}} (1 - \nu) w \ell}{72 \dot{n}_3 T_{\text{co}}^2} \frac{\Delta T_c}{T_c}. \quad (4.20)$$

To have sufficient heat exchange, the temperature of the liquid in the sinter sponge must be higher than $0.8 T_c$, the temperature of the body and of the sinter material. If we take $\Delta T_c \leq 0.05 T_c$ we find:

$$d_{sc} \leq 2 \times 10^{-7} \frac{(1 - \nu) w \ell}{\dot{n}_3 T_{co}^2} . \quad (4.21)$$

We will now show that the dependence of d_{sc} on \dot{n}_3 is only apparent. The total effective surface area of a heat exchanger is given by eq. (4.18) with

$$\sigma_{ci} = \ell w d_{sc} s \quad (4.22)$$

where s is the effective surface per unit volume of the sinter material. Assuming that the copper sponge contains per unit volume N spherical particles of diameter δ , we find for the filling factor:

$$\nu = \frac{\rho_c}{\rho_o} = N \frac{\pi}{6} \delta^3 . \quad (4.23)$$

The total effective surface per unit volume, s , equals then:

$$s = \varepsilon N \pi \delta^2 = \varepsilon \frac{\rho_c}{\rho_o} \frac{6}{\delta} = \varepsilon \nu \frac{6}{\delta} . \quad (4.24)$$

The factor ε accounts for the reduction of the surface area as a result of the formation of metal bridges between the particles, surface contamination, thermal resistance in narrow slits etc. Substitution of eqs. (4.24), (4.22) and (4.21) in eq. (4.18) shows:

$$d_{sc} \leq \frac{4 \times 10^{-3}}{T_{co}^2} \sqrt{\frac{R_K (1 - \nu)}{s}} = \frac{4 \times 10^{-3}}{T_{co}^2} \sqrt{\frac{R_K \delta (1 - \nu)}{6 \varepsilon \nu}} \quad (4.25)$$

and

$$\ell w \geq 2 \times 10^4 \dot{n}_3 \sqrt{\frac{R_K}{s(1 - \nu)}} = 2 \times 10^4 \dot{n}_3 \sqrt{\frac{R_K \delta}{6 \varepsilon \nu (1 - \nu)}} \quad (4.26)$$

The area ℓw is proportional to the flow \dot{n}_3 as could be expected and is independent of the temperature T . Only the thickness d_{sc}

increases by lowering the temperature. Hence in principle the length and width of all heat exchangers can be the same only the thickness of the sponge varies with the temperature.

In principle the eqs. (4.16), (4.25) and (4.26) give a simple prescription for the design of the sinter sponge of the concentrated side of a heat exchange.

For the dilute side the transported heat \dot{q} is proportional to $(T_c^4 - T_d^4)$ and is still determined by the temperature of the concentrated side, because $T_c^4 \gg T_d^4$. Since $T_b \approx 1.6 T_d$ we take $\Delta T_d/T_d \approx 0.5$ and we find for the thickness of the sinter material

$$d_{sd} \leq 20 \times 10^{-7} \frac{(1 - \nu) w \ell}{\dot{n}_3 T_{co}^2} = 10 d_{sc} . \quad (4.27)$$

From eqs. (4.25) and (4.27) it can be seen that especially at higher temperatures the powder layer must be thin to be effective.

Conclusions.

From eqs. (4.2) and (4.3) it can be seen that the volumes of the tubes in a dilution refrigerator are inversely proportional to $\dot{n}_3 T^{14}$. Temperatures of 2 mK have indeed been reached in rather large machines (Frossati, 1978). For lower temperatures larger machines will be necessary both with respect to volume and circulation rate.

This large circulation rate is also important for a multiple mixing chamber system in which the flow in the last mixing chamber is a certain fraction of the total flow.

For these reasons and the lack of experimental space in our old refrigerator, a new refrigerator with a circulation rate of 2.5 mmol/s has been built.

Eqs. (4.16), (4.26) and (4.27) show that the bodies of all heat exchangers can be constructed in the same way. The cross-sectional areas of the body material, the length and the width of the channels can all be equal. The only changing dimension in the configuration which depends on the temperature is the thickness of the sinter sponge.

References.

- Betts, D.S., Brewer, D.F. and Lucking, R., Proc. L.T. 13 (1972, Boulder).
- Betts, D.S. et al., J. Low Temp. Phys. 14 (1974) 331.
- Frossati, G., Thesis 1978.
- Frossati, G. and Thoulouse, D., Proc. ICEC 6, IPC Science and Techn. Press Guildford (1976) 116.
- Haeringen, W. van, Staas, F.A. and Geurst, J.A., Philips Journal of Research 34 (1979a) 107.
- Haeringen, W. van, Staas, F.A. and Geurst, J.A., Philips Journal of Research 34 (1979b) 127.
- Haeringen, W. van, Cryogenics 20 (1980) 153.
- Niinikoski, T.O., Proc. ICEC 6, IPC Science and Techn. Press Guildford (1976) 102.
- Siegwarth, J.D. and Radebaugh, R., Rev. Sci. Instrum. 43 (1972) 197.
- Staas, F.A., Weiss, K. and Severijns, A.P., Cryogenics 14 (1974) 253.
- Waele, A.Th.A.M. de, Reekers, A.B. and Gijsman, H.M., Proc. ICEC 6, IPC Science and Techn. Press Guildford (1976) 112.
- Waele, A.Th.A.M. de, Reekers, A.B. and Gijsman, H.M., Proc. 2nd Int. Symp. on Quantum Fluids and Solids, Sanibel Island, Fla, U.S.A. (1977), ed. Trickey, Adams, Dufty, Plenum Publ. Cy. (1977) 451.
- Wheatley, J.C., Vilches, D.E. and Abel, W.R., Physics 4 (1968) 1.

CHAPTER V.

THE DILUTION REFRIGERATOR WITH A CIRCULATION RATE OF 2.5 MMOL/S.

5.1 Introduction.

In this chapter a description of the 2.5 mmol/s dilution refrigerator is given.

The large flow rate provides a high cooling power, short time constants and, as has been shown in Chapter IV, gives the possibility to reach lower temperatures. It also offers a good starting point for inserting a multiple mixing chamber (Chapter VI). In order to maintain a flow rate larger than 0.5 mmol/s during long periods of time, special attention should be given to the heat exchange of the downward ^3He gas flow with the upward gas flows in the 4 K - 80 K region and to the liquid helium consumption of the 1 K plate.

The main flow resistance in the still pumping line is situated in the still orifice, which presently determines the ^3He flow at a given temperature of the still.

5.2 General description of the system.

To reduce the vibrations to the low temperature part of the system, the cryostat is hanging on a concrete block of 6000 kg, placed on air springs. All connections to the cryostat are established by flexible stainless steel bellows to reduce vibrations. The cryostat consists of 4 parts:

- a vacuum space with super isolation;
- the LN_2 container;
- a vacuum space in which contactgas can be introduced in order to reduce the cooldown time from room temperature to LN_2 temperature;
- a LHe container.

The LHe container has a diameter of 250 mm, which allows a vacuum chamber with a length of 815 mm and an inner diameter of 215 mm in which the dilution refrigerator and the associated experiments are installed.

The vacuum in the vacuum chamber is obtained by a diffusion pump (Edwards EO2) and a mechanical rotation pump (Edwards ES200).

The pumping system for the circulation of ^3He consists of a booster pump (Edwards 18B3) and a mechanical pump (Edwards ES4000). This combination is able to circulate 4 mmol/s at a pressure of about 0.07 torr (10 Pa).

To maintain large circulation rates good heat exchange in the high temperature region of the cryostat is necessary to avoid a large evaporation rate of the helium bath.

5.3 Heat exchange in the 4 K - 80 K region.

The ^3He entering the cryostat at room temperature is first precooled to 77 K (fig. 5.1) by means of a thermal ground to the LN_2 dewar. The ^3He entering the bath has a temperature T_i , which is higher than the bath temperature $T_b \approx 4.2$ K.

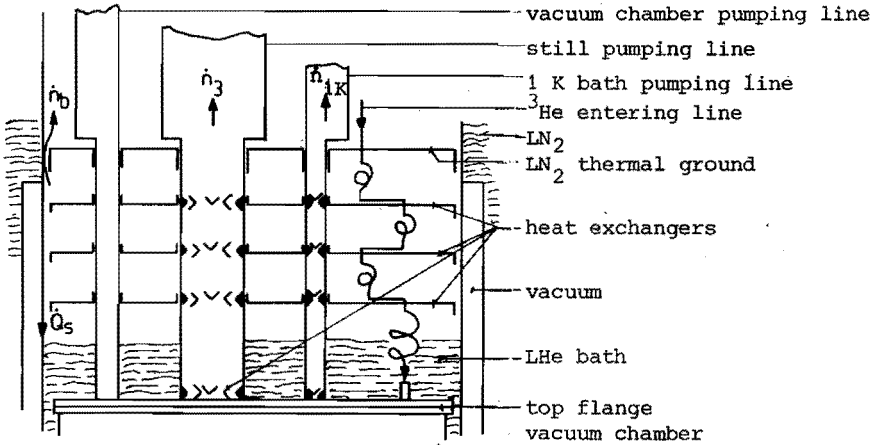


Fig. 5.1 Schematic diagram showing the heat exchangers between the cold upward streams and the warm ^3He downward stream.

The evaporation rate of the LHe bath \dot{n}_b is given by (fig. 5.2):

$$\dot{Q}_b + \dot{Q}_s - (\dot{n}_b + \dot{n}_{1K})L + \dot{n}_3 [H_3(T_i) - H_3(4.2)] = 0 \quad (5.1)$$

with L the heat of vaporization of ^4He at 4.2 K, \dot{Q}_b the heat load on the LHe bath except for the ^3He , \dot{Q}_s the heat generated inside the vacuum chamber such as in the still or to the mixing chamber, \dot{n}_{1K} the flow rate of the 1 K bath, \dot{n}_3 the ^3He flow rate and H_3

the enthalpy of ^3He . In eq. (5.1) it is assumed that \dot{n}_3 and \dot{n}_{1K} both leave the LHe bath at 4.2 K.

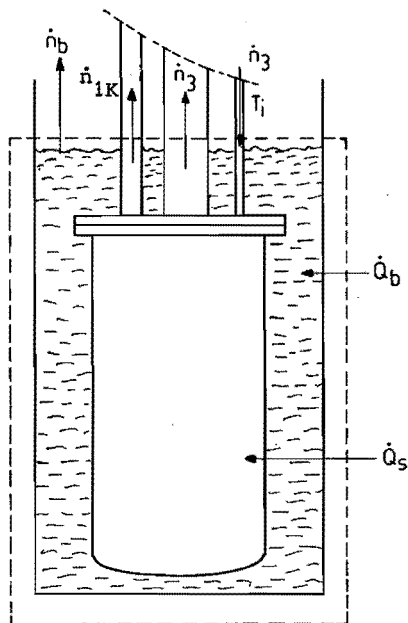


Fig. 5.2 The enthalpy balance of the total system. The dotted line indicates the (open) thermodynamic system on which the first law of thermodynamics is applied in order to derive eq. 5.1.

For $\dot{n}_3 = \dot{n}_{1K} = 0$ and $\dot{Q}_s = 0$, the static evaporation rate of the bath is 0.3 l/h or 3.2 mmol/s, corresponding to a heat load of $\dot{Q}_b = 0.26$ W. A ^3He circulation rate of 4 mmol/s with $T_i = 7$ K would cause a heat load of the same value. A value of $T_i = 77$ K would lead to a LHe evaporation of 8.4 l/h. This shows the importance of reducing T_i as far as possible and hence the necessity of introducing heat exchangers in the high temperature region of the system. To realize this heat exchange, four baffles have been inserted in the pumping lines of the 1 K bath and the still (fig. 5.3). Measurements show that the pressure drops across the baffles are negligible with regard to the total pressure

drop between the still and the booster pump. To verify the result of inserting these baffles, we measured the LHe consumption of the cryostat with $\dot{n}_3 = 4$ mmol/s, $\dot{n}_{1K} = 0$. This proved to be 0.6 l/h (or $\dot{n}_b = 5.1$ mmol/s), a small value compared to the figure of 8.4 l/h mentioned above.

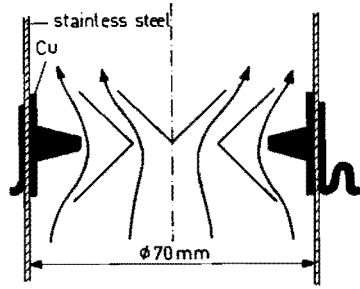


Fig. 5.3 Heat exchanger in the still pumping line.

5.4. The liquid helium consumption of the 1 K plate.

A schematic drawing of the 1 K plate and the still is given in fig. 5.4. The ^4He flows to the 1 K plate through a capillary with

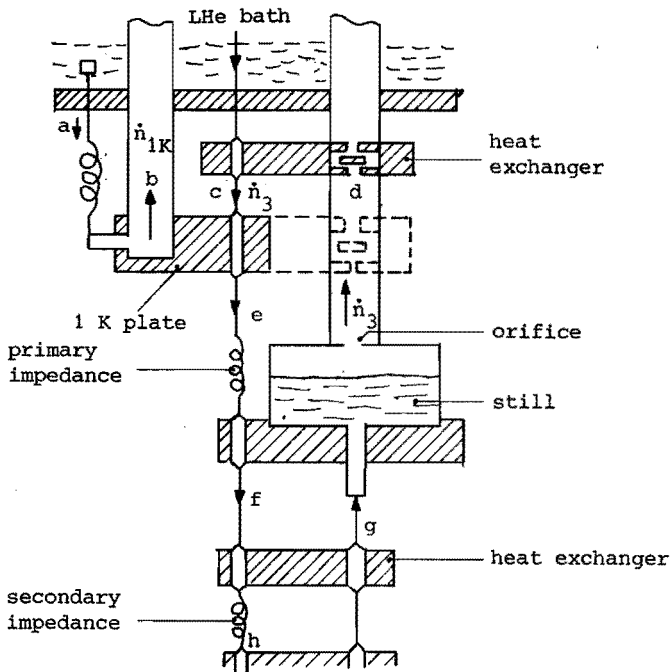


Fig. 5.4 Schematic figure of the 1 K plate, still and two heat exchangers. The T , p and H values at the points a, \dots, g are given in table 5.1.

a flow impedance $Z = 7.4 \times 10^{15} \text{ m}^{-3}$, resulting in a flow of $\dot{n}_{1\text{K}} = 3.2 \text{ mmol/s}$. As an example some typical temperatures, pressures and enthalpy values at the points indicated in fig. 5.4 are given in table 5.1 and in fig. 5.5.

	^4He		^3He				
	a	b	c	d	e	f	g
T(K)	4.2	1.7	3.2	0.7	1.7	0.7	0.2
p(kPa)	100	1.1	13	0.01	13	0.4	0.01
H(J/mol)	38.8	94.0	84	35	6	2	2

Table 5.1 Typical T, p and H values at the points of fig. 5.3.

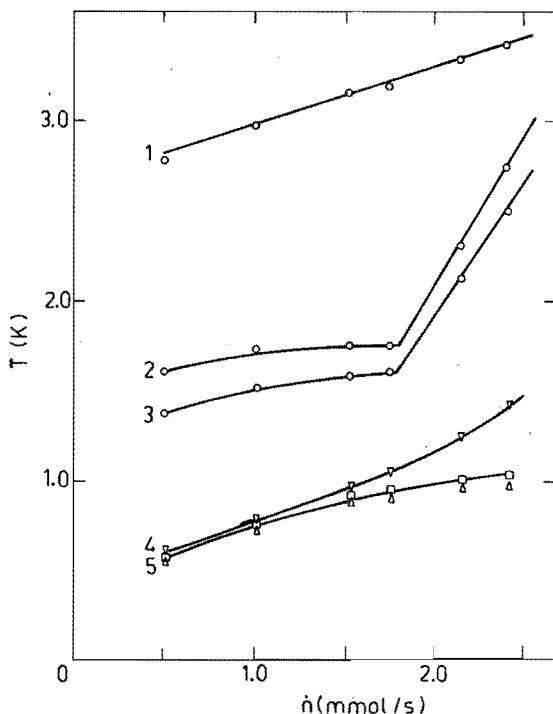


Fig. 5.5 The temperature distribution in the upper part of the dilution refrigerator vs. total flow rate.
 Line 1: temperature of the upper heat exchanger in the still pumping line.
 Line 2: temperature of the ^3He behind the 1 K bath.
 Line 3: temperature of the 1 K bath.
 Line 4: temperature of the ^3He behind the still.
 Line 5: temperature of the still plate and the still liquid.

These values are derived from tables of Radebaugh (1967), Conte (1970), Kraus (1973) and Roubeau (private communication). The enthalpy balance of the 1 K plate is:

$$\dot{Q}_{1K} + \dot{n}_{1K} H_a + \dot{n}_3 H_c = \dot{n}_{1K} H_b + \dot{n}_3 H_e \quad (5.2)$$

\dot{Q}_{1K} is the heat load, \dot{n}_{1K} the ^4He flow through the 1 K plate and \dot{n}_3 the ^3He flow. The heat exchanger between the 1 K plate and the still pumping line was not effective, so here no heat was absorbed by the vapour from the still. When $\dot{Q}_{1K} = 0$ the ^3He flow rate has a critical value \dot{n}_{3c} as a result of the critical cooling power of the 1 K plate (see for instance Delong, 1971). With the values of table 5.1 one can derive that $\dot{n}_{3c} = 0.71 \dot{n}_{1K}$. The measured value \dot{n}_{3c} was $1.8 \text{ mmol/s} = 0.56 \dot{n}_{1K}$. The difference between these values can be due to ^4He circulating with the ^3He .

5.5 Limitation of the ^3He velocity by the still orifice.

In the course of our experiments it turned out, that the temperature in the still was higher than expected. An analysis showed that the ^3He flow reaches the velocity of sound in the film-flow reducing orifice.

The first law of thermodynamics shows that the change in enthalpy of the gas between the still and in the orifice, assuming adiabatic expansion, is equal to:

$$\Delta H = \frac{\gamma}{\gamma - 1} p_s v_s \left[1 - \left(\frac{p_o}{p_s} \right)^{\frac{\gamma - 1}{\gamma}} \right] \quad (5.3)$$

with $\gamma = C_p/C_v = 1.66$ for He, p_s is the pressure in the still, v_s is the molar volume of the gas in the still and p_o is the pressure in the orifice respectively. This enthalpy difference is equal to the kinetic energy of the gas in the orifice. If D is the diameter of the orifice and \dot{n} is the molar flow rate through the orifice one can derive that:

$$\dot{n}^2 = \frac{\pi^2 D^4 p_s^2 \psi^2}{8MRT_s} \quad (5.4)$$

with M the molar mass, R the gas constant and T_s the temperature in the still. The function ψ is equal to:

$$\psi^2 = \frac{\gamma}{\gamma - 1} \left[\left(\frac{p_o}{p_s} \right)^{\frac{2}{\gamma}} - \left(\frac{p_o}{p_s} \right)^{\frac{\gamma + 1}{\gamma}} \right] \quad (5.5)$$

For $p_o/p_s = \left(\frac{2}{\gamma + 1} \right)^{\frac{\gamma}{\gamma - 1}}$ the function ψ has a maximum value ψ_m

$$\psi_m = \left(\frac{2}{\gamma + 1} \right)^{\frac{1}{\gamma - 1}} \sqrt{\frac{\gamma}{\gamma + 1}} \quad (5.6)$$

For helium $\psi_m = 0.51$. In fig. 5.6 ψ is given as a function of p_o/p_s . The dotted part of the graph has no physical meaning. The

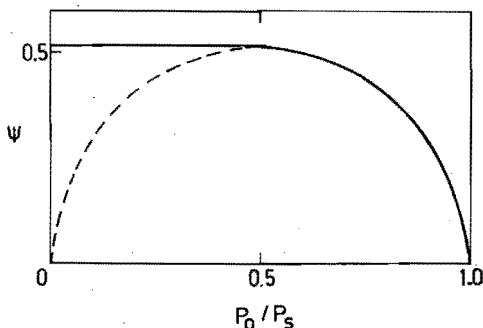


Fig. 5.6 The function ψ , which is proportional to the flow rate vs. the pressure coefficient p_o/p_s , with p_o the pressure in the still and p_s the pressure in the orifice respectively. The dotted part of the graph has no physical meaning.

velocity of the gas in the orifice at p_o/p_s , corresponding to the maximum of the curve, is equal to the velocity of sound at temperature T_o , as can be calculated from eqs. (5.3) - (5.6) and the fact that for adiabatic expansion $T_o = T_s (p_o/p_s)^{(\gamma - 1)/\gamma}$. For p_o/p_s values below the maximum a reduction of the pressure behind the orifice does not lead to an increase of \dot{n} . The orifice constitutes a large flow resistance.

In order to investigate this effect we measured the temperature flow relation with pure ^4He (fig. 5.7).

The vapour pressure in this temperature region $0.6 \text{ K} < T < 1.0 \text{ K}$ fits the relation:

$$p_s = p_{4\text{He}} \approx 1.22 \times 10^5 \exp(-9/T_s) . \quad (5.7)$$

The limiting value for the ^4He flow can be calculated with eq. (5.4) and is given by:

$$\dot{n}_4 = 4.2 D^2 p_s / \sqrt{T_s} \quad (5.8)$$

where D is the diameter of the orifice, p_s and T_s the pressure and temperature in the still respectively. With eq. (5.7) a T_s vs. \dot{n}_4 dependence can be derived which is in good agreement with the measured values (fig. 5.7).

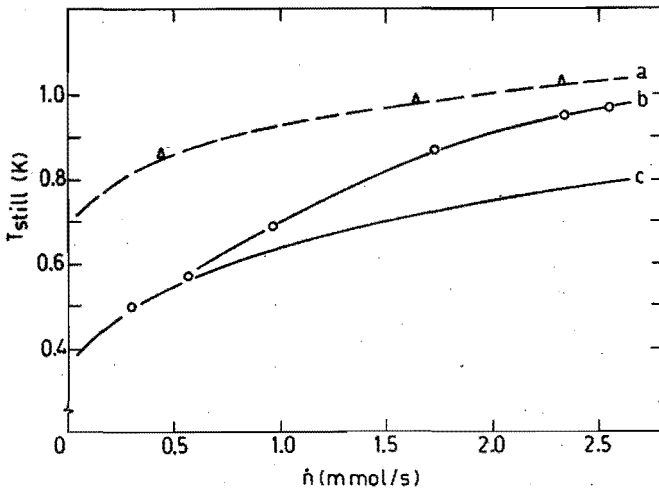


Fig. 5.7 Dependence of the still temperature vs. flow rate for several different experimental situations:

Δ : measured with pure ^4He .

\circ : measured with the dilution refrigerator in operation.

Line a: assuming pure ^4He flow.

Line b: is for visual aid only.

Line c: assuming pure ^3He flow.

We can also apply eq. (5.4) to the ^3He circulation. The limiting value is then given by:

$$\dot{n}_3 = 3.6 D^2 p_s / \sqrt{T_s} \quad (5.9)$$

In the temperature region $0.6 \text{ K} < T_s < 0.8 \text{ K}$, p_s is given by (Radebaugh, 1967):

$$p_s \approx 705 \exp(-3/T_s) . \quad (5.10)$$

With this relation, eq. (5.9) gives T_s and p_s dependences on \dot{n}_3 (fig. 5.7). In this figure, also the measured values are reported. At low flows a good agreement is obtained, whereas at higher flow rates the amount of ^4He plays an important role.

Up to now the flow is limited to 2.5 mmol/s. A larger flow rate would require a higher still temperature resulting in a too large amount of ^4He circulating with the ^3He . The diameter of the orifice has to be larger to get the flow rate of 4 mmol/s, which is the flow rate permitted by the other components of the still pumping system.

5.6 The construction and performance of the heat exchangers.

In our machine 10 Niinikoski type heat exchangers with an open passage for the liquids are employed (fig. 5.8). The heat exchangers are machined from a copper block. In the two circular channels, one for the dilute and one for the concentrated side, first a small layer of copper powder (produced by the Norddeutsche Affinerie, Hamburg, type FL) with an average grain size of $5.0 \mu\text{m}$ and a specific area of about $1300 \text{ cm}^2/\text{g}$, is sintered at a temperature of 900°C for one hour, to get a rough surface for the next sintering. In order to provide a free channel for the liquid and to ensure that the calculated amount of copper powder sticks to the walls, the powder is hammered with a piston around a teflon spacer in the center of the channels. In this way we obtained a packing factor of 30%. Subsequently the exchanger is installed in an oven and evacuated for about 1 hour to remove all the air inside the pores. Then powder is sintered for 1 hour in a 8% hydrogen/92% nitrogen atmosphere at a temperature of 300°C . After the sintering the teflon spacer, which is a little conical, is removed and a brass spacer is submitted in the center of the concentrated side in order to reduce the ^3He content. This spacer is designed in such a way that an open channel remains for the liquid. Finally four German silver caps are soft soldered to the

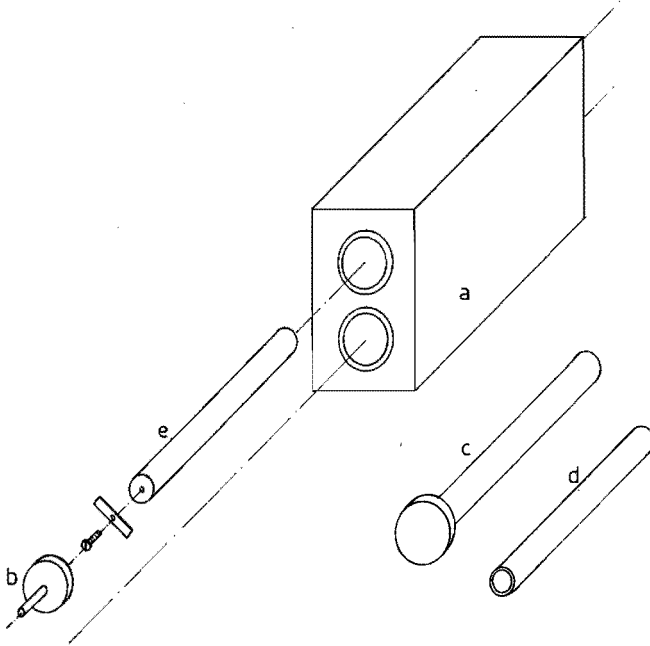


Fig. 5.8 Components for a heat exchanger.

- a. Copper block.*
- b. 4 German silver connections for tubes;
will be soldered to a.*
- c. 2 teflon spacers.*
- d. Piston to hammer copper powder.*
- e. Brass filling spacer with connections.*

copper exchanger. The heat exchangers are able to withstand a pressure of 50 atm which is used for leak testing.

The total amount of copper powder in our machine is about 90 grammes. Calculated from the grain size this corresponds to 12 m^2 .

In fig. 5.9 the minimum entrance temperature at several flows has been given. The cubic behavior of the temperature vs. the ^3He flow is in good agreement with eq. (4.14). Calculating the reduction factor ϵ with a Kapitza coefficient of $R_K = 0.02 \text{ m}^2 \text{ K}^4 / \text{W}$ and a surface of 12 m^2 we find $\epsilon = 0.10$. In this calculation a correction is made for the fact that our heat exchangers are not continuous (Staas, 1974) and each give a temperature reduction of 25%. Hence the efficiency of the heat exchanging surface is

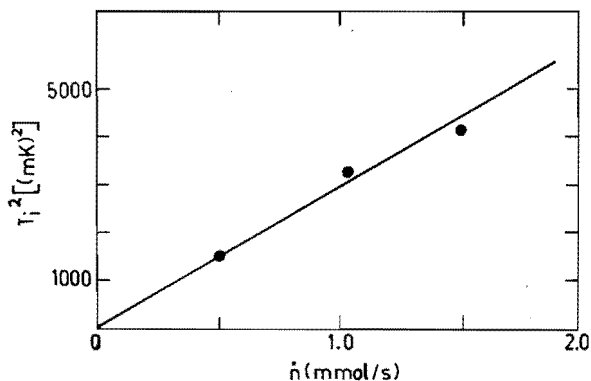


Fig. 5.9 The measured minimum entrance temperature vs. the flow rate. The calculated surface σ is 0.7 m^2 with $R_K = 0.02 \text{ m}^2 \text{ K}^4 / \text{W}$.

rather low. The same observation was made by Radebaugh et al. (1971) and Frossati (1978).

In fig. 5.10 the cooling power of the mixing chamber is given for

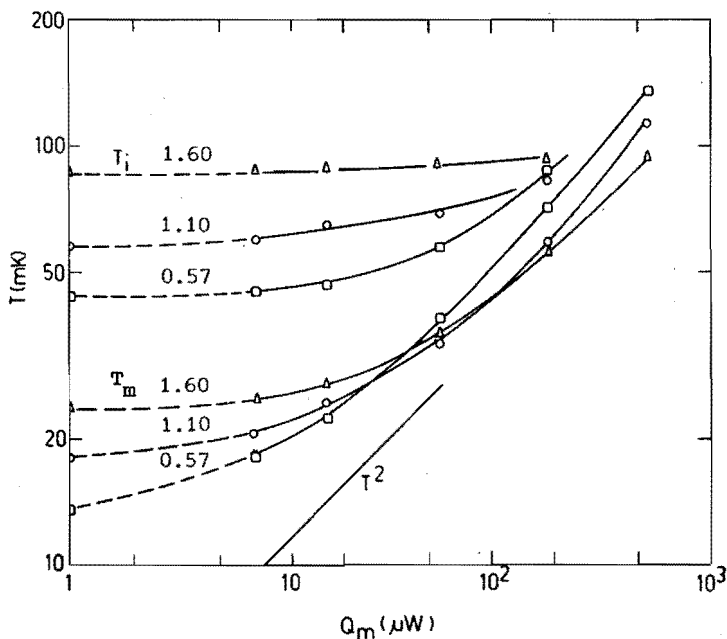


Fig. 5.10 Cooling power measurements of a single mixing chamber (T_m) for $\dot{h}_3 = 0.57$; 1.10; 1.60 mmol/s respectively. Also the temperatures (T_i) of the ^3He entering the mixing chamber are given. This cooling power is measured as described in Ch. VII.

$\dot{n}_3 = 0.57, 1.10$ and 1.60 mmol/s respectively. Since $T \approx 18$ mK for $\dot{n}_3 = 1.10$ mmol/s this set-up provides a good starting point for a further reduction of the temperature by installation of a multiple mixing chamber. This cooling power is measured as described in Chapter VII.

References.

- Conte, R.R., Elements de Cryogénie, ed. Masson et Co (1970).
- Delong, L.E., Symko, O.G., Wheatley, J.C., Rev. Sci. Instr. 42 (1971) 147.
- Frossati, G., Proc. of the 15th LT conf., Journal de Physique (Paris), Colloq. C-6, suppl. 8 (1978) 1578.
- Kraus, J., Thesis München.
- Laumond, Y., thesis, Grenoble (1972), unpublished.
- Radebaugh, R., NBS Technical Note 362 (1967).
- Radebaugh, R. and Siegwarth, J.D., Phys. Rev. Lett. 27 (1971) 796.
- Roubeau, private communication.
- Staas, F.A., Weiss, K., Severijns, A.P., Cryogenics 14 (1974) 253.
- Zucrow, M.J. and Hoffman, J.D., Gas Dynamics, vol. I, Wiley and Sons, Inc. New York.

CHAPTER VI.

THE MULTIPLE MIXING CHAMBER (THEORY).

6.1 Introduction.

The multiple mixing chamber has been developed in our laboratory (De Waele et al., 1976a, 1976b, 1977, 1978; Coops et al., 1979). Since the first successful attempts, it has been studied by several groups (Frossati, 1977, 1978; Polturac, 1977, 1979; Schumacher, 1978; SHE Company, private communication). The group in Grenoble observed temperatures down to 2.8 mK with a double mixing chamber with a total flow rate of 600 $\mu\text{mol/s}$ and a relatively small heat exchanger. Polturac et al. measured the cooling power and the influence of Z_1 (fig. 6.1).

In this chapter we will discuss the parameters which are important for a double mixing chamber system. The advantages and disadvantages of such a system in comparison with a conventional mixing chamber will also be discussed.

In the last part of this chapter we will describe the relations of a triple mixing chamber.

In the calculations we use the low-temperature approximations for viscosity, thermal conductivity, enthalpy etc.

Parts of this chapter have already been published (Coops, 1979).

6.2.1 The double mixing chamber.

A schematic diagram of a Double Mixing Chamber (DMC) is given in fig. 6.1. In the double mixing chamber a flow of ^3He in the

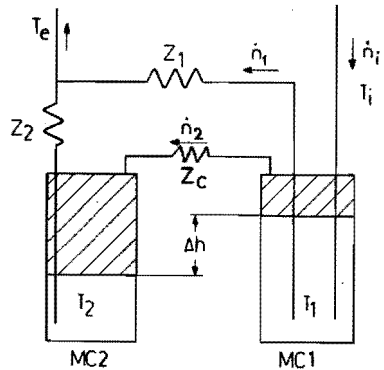


Fig. 6.1 Schematic diagram of a double mixing chamber.

concentrated phase is cooled in the first mixing chamber (MC1) before it enters the second chamber (MC2).

The flow distribution is controlled by the impedances Z_1 and Z_2 at the outlet of the mixing chambers.

The equations describing the temperatures in the stationary state are:

$$\dot{Q}_1 + 12 \dot{n}_1 T_1^2 = 96 \dot{n}_1 T_1^2 + 12 \dot{n}_2 T_1^2 ; \quad (6.1)$$

$$\dot{Q}_2 + 12 \dot{n}_2 T_1^2 = 96 \dot{n}_2 T_2^2 ; \quad (6.2)$$

$$\Pi_0 (T_1^2 - T_2^2) = Z_1 \frac{\eta_d}{T_1^2} \dot{n}_1 V_d - Z_2 \frac{\eta_d}{T_2^2} \dot{n}_2 V_d ; \quad (6.3)$$

$$\dot{n}_i = \dot{n}_1 + \dot{n}_2 . \quad (6.4)$$

The symbols are explained in fig. 6.1; \dot{Q}_1 and \dot{Q}_2 are the total heat loads, including viscous heating and conducted heat, $\Pi_0 T^2$ is the temperature-dependent term in the osmotic pressure along the phase separation curve. The eqs. (6.1) and (6.2) are derived from the enthalpy balance. The eq. (6.3) is obtained assuming $\nabla \mu_4 = 0$, hence $p - \Pi$ is constant in Z_1 and Z_2 .

6.2.2 The value of Z_2 .

It is preferable to design a DMC in such a way that the second term in the right hand side of eq. (6.3) is negligible ($Z_2 \approx 0$) because it causes $T_2 > T_1$ for large values of \dot{Q}_2 . In order to illustrate this point we consider the case that in an existing dilution refrigerator a SMC is replaced by a DMC. As we will show further on, the temperature T_1 hardly changes by this operation. We will assume that the total heat load remains unchanged ($\dot{Q}_m = \dot{Q}_1 + \dot{Q}_2$). With these conditions it can be derived from the enthalpy balance of a single mixing chamber:

$$\dot{Q}_m + 12 \dot{n}_i T_1^2 = 96 \dot{n}_i T_m^2 \quad (6.5)$$

and from eqs. (6.1), (6.2) and (6.4) that

$$\dot{n}_1 T_1^2 + (\dot{n}_i - \dot{n}_1) T_2^2 = \dot{n}_i T_m^2 \quad (6.6)$$

since $0 \leq \dot{n}_1 \leq \dot{n}_i$ one obtains

$$0 \leq \frac{T_m^2 - T_2^2}{T_1^2 - T_2^2} \leq 1 \quad (6.7)$$

resulting in:

$$T_2 \leq T_m \leq T_1, \quad (6.8)$$

or

$$T_2 \geq T_m \geq T_1. \quad (6.9)$$

Hence, T_1 and T_2 cannot be both smaller than T_m , the temperature of the single mixing chamber under the same conditions. To avoid the undesirable solution (6.9) the impedance Z_2 should be so small that the second term in the right hand side of eq. (6.3) can be neglected.

With $Z_1 \dot{n}_1 \tilde{\eta}_d V_d \approx \Pi_0 T_1^4$ this condition gives:

$$Z_2 \ll \Pi_0 V_d T_2^2 T_1^2 / (\eta_d \dot{n}_2 V_d^2). \quad (6.10)$$

The outlet tube of MC2 must also satisfy the usual condition of small viscous heating (chapter 4.2.2):

$$Z_2 \ll 54 T_2^4 / (\eta_d \dot{n}_2 V_d^2). \quad (6.11)$$

When this condition is satisfied, condition (6.10) is automatically met since $T_1 > T_2$ and $\Pi_0 V_d = 43 \text{ J/molK}^2$.

6.2.3 Dimensionless form of the equations.

It is convenient to bring the above mentioned eqs. (6.1) - (6.5) in a reduced form, using:

$$t_k = \frac{T_k}{T_i}, \quad r = \frac{\dot{n}_1}{\dot{n}_i}, \quad A_k = \frac{512}{7} \frac{Z_k \eta_d \dot{n}_i V_d}{\Pi_0 T_i^4}$$

and

(6.12)

$$q_k = \frac{\dot{Q}_k}{12 \dot{n}_i T_i^2} \quad (k = m, 1, 2).$$

The equations then read with $\dot{n}_2 = (1 - r)\dot{n}_i$:

$$q_m + 1 = 8 t_m^2; \quad (6.13)$$

$$q_1 + 1 = (7r + 1)t_1^2; \quad (6.14)$$

$$q_2 = (1 - r)(8 t_2^2 - t_1^2); \quad (6.15)$$

$$t_1^2 - t_2^2 = \frac{7}{512} \left(\frac{A_1 r}{t_1^2} - \frac{A_2 (1 - r)}{t_2^2} \right). \quad (6.16)$$

The condition (6.10) then becomes:

$$A_2 \ll \frac{512}{7} \frac{t_2^2 t_1^2}{(1-r)}. \quad (6.17)$$

To illustrate the behaviour of a DMC when condition (6.17) is not met, we plot a solution of these equations in fig. 6.2, where with increasing q_2 the temperature of MC2 becomes higher than that of MC1, and hence also higher than the temperature of a SMC with the same heat load. For the rest of this thesis we therefore assume condition (6.10) (and thus also (6.11) or (6.17)) to be satisfied and we rewrite eq. (6.16) in the simplified form:

$$t_1^2 - t_2^2 = \frac{7}{512} \frac{A_1 r}{t_1^2}. \quad (6.18)$$

The typical properties of a DMC are determined by the parameter A_1 defined in eq. (6.12). Its value increases with decreasing inlet temperature. At high temperatures, i.e. $A_1 \ll 1$, the temperatures $T_1 \approx T_2 \approx T_m$ and the DMC behaves as one single mixing chamber. This property can be observed during cooldown. When $A_1 \approx 1$, one obtains $T_i > T_1 > T_m > T_2$. For $A_1 \gg 1$ the solutions tend to $\dot{n}_1 = 0$, $T_1 = T_i$ and $T_2 = T_m$,

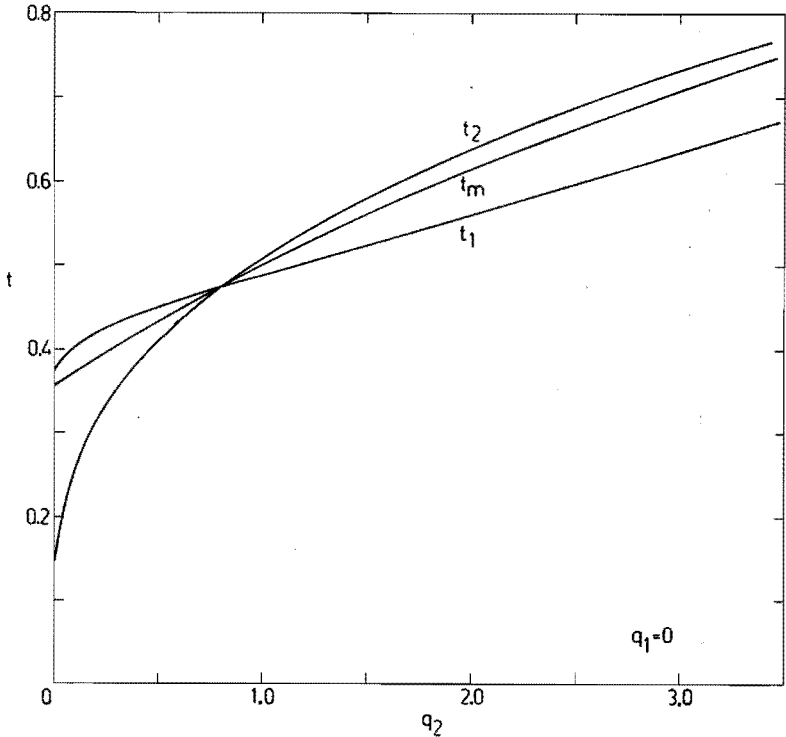


Fig. 6.2 Dependences of the reduced temperatures t_1 , t_2 and t_m on the reduced heating power. In this figure a solution is given for $A_1 = A_2 = 9.6$. The limiting value of $q_2 = 7$. In that case $t_1 = t_2 = t_m = 1$ and $r = 0$.

i.e. the temperature of MC2 is equal to the temperature of a single mixing chamber. For optimum performance of a DMC A_1 should be of the order of one.

For a given value of q_2 the reduced temperature t_1 and t_2 and the flow rate r are functions of A_1 (see fig. 6.3). As can be seen from fig. 6.3a, the minimum t_2 for a given q_2 is fairly independent of A_1 (this means independent of Z_1 or \dot{n}_1). A value of A_1 in the region 2-10 is a good value resulting in $r \approx 0.5$ and $t_2 \approx 0.2$ for the lower q_2 values.

6.2.4 Height of the mixing chambers.

It is possible to construct the DMC in such a way that the phase boundaries are inside the mixing chambers at all temperatures.

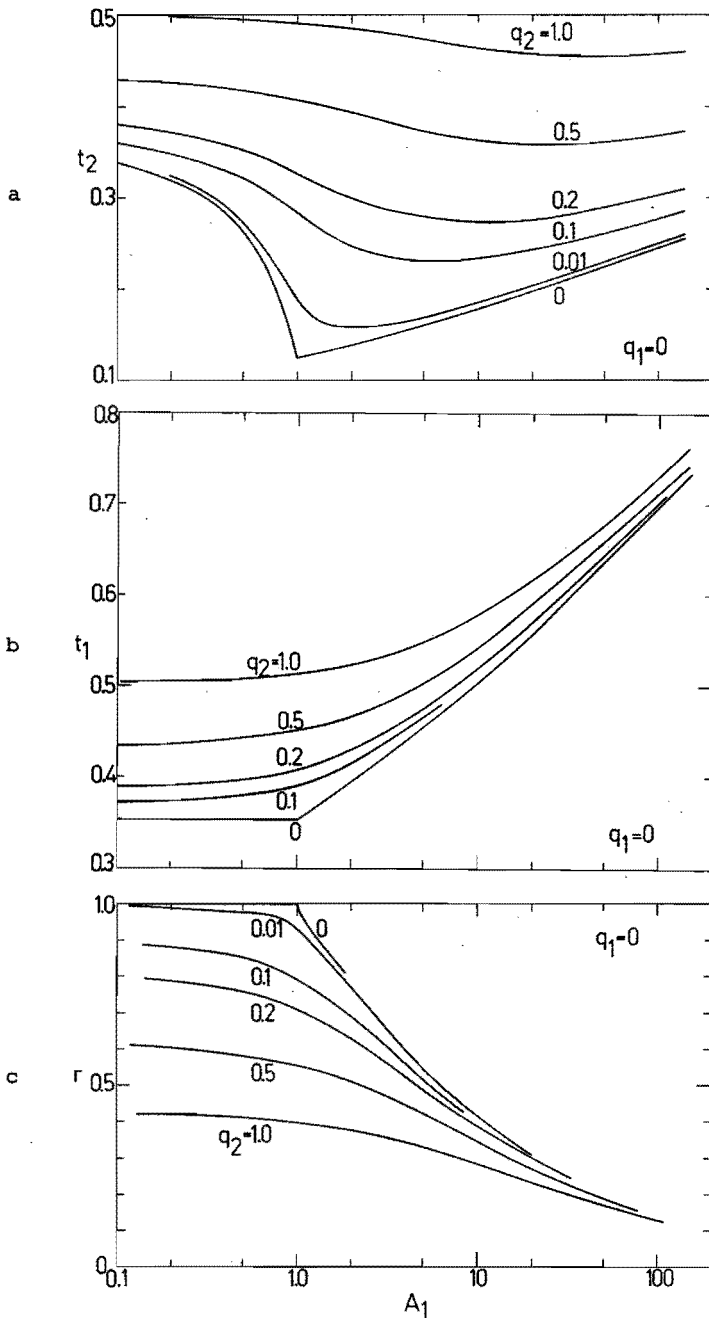


Fig. 6.3 The behaviour of a DMC as a function of A_1 with $q_1 = 0$. Curves are given for several heat loads q_2 . The values of t_2 near the minimum are fairly independent of A_1 . a: The reduced temperature of MC2. b: The reduced temperature of MC1. c: The relative flow through MC1.

The difference in height between the phase boundaries, Δh , is given by the relation:

$$\Delta\rho \cdot g \cdot \Delta h = \Pi_0 (T_1^2 - T_2^2) - Z_c \frac{\eta_c}{T_1^2} \dot{n}_2 V_c , \quad (6.19)$$

where Z_c is the impedance of the tube connecting the two mixing chambers, $\Delta\rho$ the difference of the densities of the dilute and concentrated phases and g the gravitational acceleration ($g \approx 9.81 \text{ m/s}^2$). For the other symbols compare eq. (6.3). The value of Δh for $\dot{Q}_1 = \dot{Q}_2 = 0$ and $Z_c = 0$ are given by:

$$\Delta h = 3.0 \times 10^{-13} \frac{Z_1 \dot{n}_1}{T_i^2} \quad \text{for } A_1 \leq 1 . \quad (6.20a)$$

$$\Delta h \approx 5.0 \times 10^{-4} (Z_1 \dot{n}_1 T_i^2)^{1/3} \quad \text{for } 1 \leq A_1 \leq 20. \quad (6.20b)$$

The largest value of Δh , Δh_{\max} , is found when $A_1 = 1$. In that case the two solutions for Δh , given by (6.20a) and (6.20b) are equal. Eliminating T_i yields:

$$\Delta h_{\max} = 2.5 \times 10^{-6} \sqrt{Z_1 \dot{n}_1} . \quad (6.21)$$

The $\Delta h - T_i$ dependence is illustrated in fig. 6.4, where we have chosen a situation where $A_1 = 1$ at $T_i = 40 \text{ mK}$.

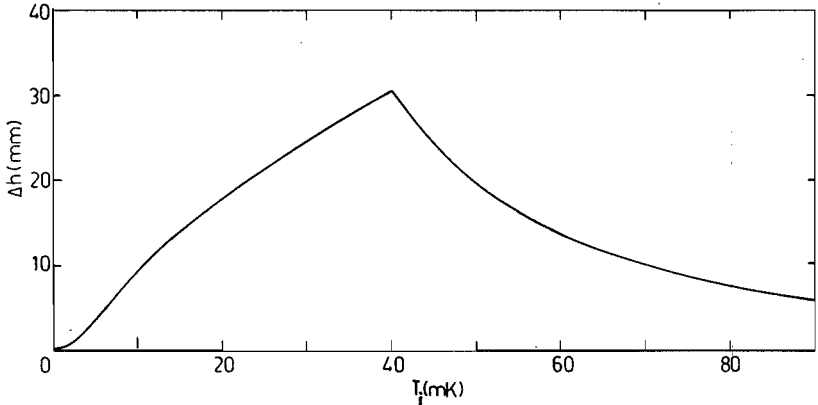


Fig. 6.4 The difference in height between the phase boundaries in a DMC; $A_1 = 1$ when $T_i = 40 \text{ mK}$. The DMC has to be designed in such a way that at this temperature the phase boundaries are inside the MC's.

The systems must be designed in such a way that the phase boundaries are inside the mixing chambers at the maximum, given by eq. (6.21). Hence Δh_{\max} is the minimum height the mixing chambers should have if their tops are at equal height.

6.2.5 The dilute exit temperature of a double mixing chamber system.

We now consider a double mixing chamber system in stationary operation, with $T_2 < T_1$. The osmotic pressure in the return line is equal to that in MC2 and lower than in MC1. The dilute ^3He leaving the first chamber is "throttled" in the impedance Z_1 to this lower osmotic pressure.

This process results in an increase in temperature (viscous heating). As a result the temperature in the return line of a DMC is always higher than T_2 . To calculate this outlet temperature T_e we use the expression for the enthalpy of dilute ^3He under constant osmotic pressure:

$$H_{\pi} = 54 T^2 + 42 T_2^2, \quad (6.22)$$

which is based on $H_{\text{sat}} = 96 T^2$ along the phase separation curve and on $C_{\pi} = (\partial H / \partial T)_{\pi} = 108 T$.

The enthalpy balance of a DMC without heat load can thus be written as:

$$12 T_1^2 = 54 T_e^2 + 42 T_2^2, \quad (6.23)$$

and for the single mixing chamber:

$$12 T_1^2 = 96 T_m^2. \quad (6.24)$$

From these equations and from eqs. (6.13) - (6.15) follows that:

$$\left(\frac{T_e}{T_m}\right)^2 \approx \frac{12 r + 1}{7 r + 1}, \quad (6.25)$$

thus:

$$T_m \leq T_e \leq 1.3 T_m. \quad (6.26)$$

The temperature T_e of the ^3He in the return line of a DMC is thus always higher than in the case of a SMC with the same inlet temperature. In the case $r = 1$ than $T_e = 1.3 T_m$.

The heat exchange in the coldest part of the heat exchanger is determined by $T_i^4 - T_m^4 = 0.98 T_i^4$ in the SMC and by $T_i^4 - T_e^4 = 0.96 T_i^4$ in the DMC case (when we take $T_i \approx 2.8 T_m$). This result shows that T_i hardly changes when in an existing dilution refrigerator the SMC is replaced by a DMC.

The temperature of the liquid in the impedance Z_1 rises from T_1 at the entrance to $1.3 T_1$ at the end assuming $A_1 \geq 1$ and $\dot{Q}_2 = 0$. The corresponding decrease in viscosity reduces the effective value of the impedance in eqs. (6.3) or (6.12) with about 25%. However, this reduction of Z_1 hardly influences the temperature of the DMC system. We therefore have neglected this correction in the low temperature region.

6.3 The construction of a DMC system.

Using the foregoing results we will, as an example, calculate the parameters of a DMC system, to be inserted in a dilution refrigerator that, with a SMC, obtained an entrance temperature of the mixing chamber $T_i = 60$ mK at a flow rate of 1 mmol/s.

The impedance Z_1 .

To calculate the size of the impedance Z_1 we use eq. (6.12). With $T_i = 60$ mK and $A_1 = 2$, a value of $Z_1 = 1.65 \times 10^{12} \text{ m}^{-3}$ is found. Supposing laminar flow $Z_1 = 128 l/\pi d^4$. According to this, we can choose a tube of convenient sizes, for instance with a diameter $d = 1.8$ mm and a length $l \approx 40$ cm. As is shown above (e.g. fig. 6.3) the performance of a DMC is not critically dependent of the particular choice of Z_1 . This property facilitates the construction of a DMC.

Height of the mixing chambers.

From eq. (6.21), with the above-mentioned Z_1 and \dot{n}_i values, one obtains $\Delta h_{\text{max}} = 10.2$ cm. In our experiments the heights of the mixing chambers were generally of the order of 12 cm.

The input line of MC1.

To obtain the lowest temperature possible, we have to minimize heat conduction and viscous heating. The tube entering a MC has to satisfy the relation (chapter IV):

$$2.4 \times 10^{-5} \frac{d^2}{\dot{n}_i T_i^2} \ll 1 \ll 10^{15} \times \frac{T_i^4 d^4}{\dot{n}_i} , \quad (6.27)$$

where d is the diameter and l the length of the input line. With $T_i = 60$ mK, $\dot{n}_i = 1$ mmol/s and $d \approx 0.8$ mm eq. (6.27) shows:

$$4.3 \times 10^{-6} \text{ m} \ll 1 \ll 5.3 \text{ m} .$$

We therefore choose a tube with a diameter $d \approx 0.8$ mm and a length $l < 1$ m.

The tube connecting MC1 and MC2.

Because the tube connecting MC1 and MC2 contains concentrated ^3He it also has to satisfy eq. (6.27). We have to replace T_i by T_1 and \dot{n}_i by $\dot{n}_2 \approx 0.5 \dot{n}_i$.

In order to be sure that the phase boundaries are in the proper position the following condition has to be satisfied:

$$\Pi_o T_1^2 \gg \frac{\eta_c}{T_1^2} Z_c \dot{n}_2 V_c , \quad (6.28)$$

which means that the osmotic pressure difference between MC1 and MC2 has to be much larger than the pressure drop in Z_c . Condition (6.28) yields

$$1 \ll 0.3 \times 10^{15} \frac{T_1^4 d^4}{\dot{n}_2} . \quad (6.29)$$

The conditions (6.27) and (6.29) are both satisfied when:

$$2.4 \times 10^{-5} \frac{d^2}{\dot{n}_2 T_1^2} \ll 1 \ll 0.3 \times 10^{15} \frac{T_1^4 d^4}{\dot{n}_2} . \quad (6.30)$$

With a diameter $d \approx 1.8$ mm, $T_1 = 30$ mK and $\dot{n}_2 \approx 0.5$ mmol/s one finds:

$$1.7 \times 10^{-4} \text{ m} \ll 1 \ll 5.1 \text{ m} .$$

If we take e.g. $1 < 1 \text{ m}$, eq. (6.30) is fairly well satisfied.

The exit tube of MC2.

To minimize the heat conduction and viscous heating in the dilute output tube of MC2 we take the approximation we obtained in chapter IV:

$$0.44 \times 10^{-5} \frac{d^2}{\dot{n}_2 T_2^2} \ll 1 \ll 0.15 \times 10^{15} \frac{T_d^4 d^4}{\dot{n}_2} . \quad (6.31)$$

For $T_2 \approx 10 \text{ mK}$ and $\dot{n}_2 \approx 0.5 \text{ mmol/s}$ this condition is satisfied with $d \approx 5 \text{ mm}$ and $l \approx 10 \text{ cm}$.

6.4 Comparison between a single and a multiple mixing chamber system.

In this paragraph we compare the single mixing chamber and the double mixing chamber in five different cases of experimental interest.

For simplicity we assume that in the DMC about 50% of the ^3He is diluted in MC1, giving a temperature reduction of a factor 2. Also assuming that (eq. (4.14))

$$\sigma T_i^2 \approx 96 R_K \dot{n}_i \quad (6.32)$$

holds, we are able to draw conclusions in the five following cases.

1. The systems have the same total flow rate and the same area in the heat exchangers.

This is usually the case when one does not change the parts in the refrigerator above the mixing chamber (heat exchangers, pumping system). According to eq. (6.32) the systems have the same T_i , so the lowest temperature of a DMC is a factor 2 lower than the one of a SMC. Accordingly the cooling power of a DMC is larger. At high temperatures the DMC behaves as a SMC and the cooling powers are equal. It is preferable to use a DMC. This behaviour will be illustrated in chapter VII.

2. The systems have the same minimum temperature and the same low-temperature cooling power.

This case is important when a system has to be designed for a certain low-temperature performance and the pumps and heat exchangers can be chosen freely.

Since 50% of the total flow is diluted in MC2 we need for the same cooling power at low temperatures twice the flow of a SMC. On the other hand we can allow an incoming temperature T_1 for a DMC which is twice as high. According to eq. (6.32) the surface area is half the area needed for a SMC. The amount of ^3He can be smaller accordingly. At high temperatures we have a cooling power which is twice the cooling power of a SMC. Hence, in the case of a DMC larger pumps and smaller heat exchangers are needed to satisfy the requirements. It depends on the situation which of the two methods is preferable. For very low temperatures or high flow rates a DMC might be advisable, to avoid too large heat exchangers.

3. The systems have the same minimum temperature and the same (total) flow rate.

This is the case when a certain minimum temperature is desired while limitations are determined by the pumps or the pumping lines and e.g. not by the disposable amount of ^3He . Having the same minimum temperature, the temperature T_1 of the incoming ^3He of a DMC can be twice as high as in a SMC. Having the same flow rate, eq. (6.32) says we have to use 4 times more surface area of the heat exchangers in the SMC configuration (hence 4 times more ^3He in the heat exchangers). The cooling power at low temperatures for SMC is now 2 times that of a DMC, because the flow into MC2 is reduced by 50%. The cooling powers at high temperatures are equal because the two systems have the same total flow rate. Under these circumstances a SMC is preferable.

4. The systems have the same minimum temperature and the same exchange area.

This case is important when a certain minimum temperature is desired and the number of heat exchangers is fixed (e.g. due to

lack of space) while the circulation rate can be varied. Again we have in the DMC configuration an inlet temperature which is twice the value in a SMC. Therefore the flow rate can be 4 times larger. The cooling power of a DMC at low temperatures is thus 2 times larger. At high temperatures the cooling power is 4 times the one of a SMC. In this case a DMC should be used.

5. The optimum cooling power of a single and a double mixing chamber.

From the enthalpy balance of a single mixing chamber (eq. (6.5)) and eq. (6.32) one can find the optimum cooling power \dot{Q}_{mo} at a given temperature and with a given heat exchanger configuration by optimizing with respect to the total flow rate \dot{n}_1 . The result is $\dot{Q}_{mo} = (\sigma/96 R_K) T_m^4$.

A similar type of calculation can also be performed with a DMC (eqs. (6.1) - (6.4)) and eq. (6.32). Optimizing the cooling power at a given temperature with respect to Z_1 and \dot{n}_1 gives

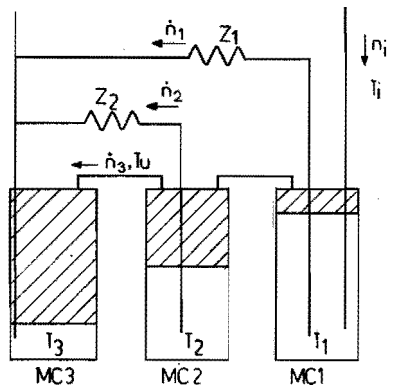
$$\dot{Q}_{20} = \frac{16}{7} (\sigma/96 R_K) T_2^4.$$

Hence the optimum cooling power of a DMC at a given temperature is more than 2 times the cooling power of a SMC.

6.5 The triple mixing chamber.

The equations describing the triple mixing chamber (fig. 6.5) in the stationary state, neglecting the impedance in the concentrated lines, are analogous to the equations of a double mixing chamber.

Fig. 6.5 Schematic diagram of a triple mixing chamber, neglecting the impedance in the outlet tube of MC3.



Here one has 3 equations for the enthalpy balances and two equations for the flows through Z_1 and Z_2 .

$$\dot{Q}_1 + 12 \dot{n}_1 T_1^2 = 12(\dot{n}_i - \dot{n}_1) T_1^2 + 96 \dot{n}_1 T_1^2 \quad (6.33)$$

$$\dot{Q}_2 + 12(\dot{n}_i - \dot{n}_1) T_1^2 = 12(\dot{n}_i - \dot{n}_1 - \dot{n}_2) T_2^2 + 96 \dot{n}_2 T_2^2 \quad (6.34)$$

$$\dot{Q}_3 + 12(\dot{n}_i - \dot{n}_1 - \dot{n}_2) T_2^2 = 96(\dot{n}_i - \dot{n}_1 - \dot{n}_2) T_3^2 \quad (6.35)$$

$$\Pi_0 (T_1^2 - T_3^2) = \frac{Z_1 \eta_d \dot{n}_1 v_d}{T_1^2} \quad (6.36)$$

$$\Pi_0 (T_2^2 - T_3^2) = \frac{Z_2 \eta_d \dot{n}_2 v_d}{T_2^2} \quad (6.37)$$

In fig. 6.6 an example of a numerical solution of the equations is given. The figure shows that the value of T_3 near the minimum does not depend strongly on Z_1 or Z_2 . The values of Z_1 and Z_2 can be varied by an order of magnitude without changing T_3 significantly.

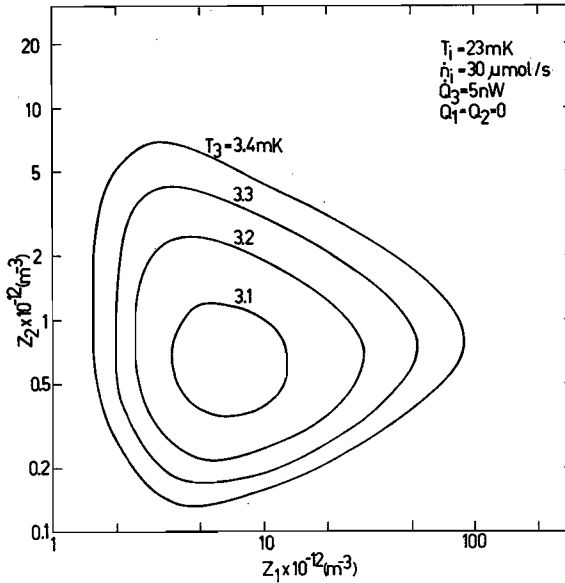


Fig. 6.6 Contours of constant T_3 in the Z_1 - Z_2 plane of a triple MC system.

The ^3He flowing into MC3 would acquire the temperature T_2 of the phase boundary of MC2 as good as possible. It is not permitted to extend the entrance tube into the dilute phase because hydrostatic pressure differences may prevent a proper flow distribution in the system. The ^3He has to pass MC2 through the concentrated phase, at some distance h from the phase boundary (with surface area S). The temperature T_u of the ^3He leaving MC2 will be higher than T_2 .

The temperature distribution in the mixing chamber can be calculated from the differential equation:

$$\frac{SK_c}{T} \frac{dT}{dh} + 12 \dot{n}_2 T^2 = \text{constant} = 96 \dot{n}_2 T_2^2. \quad (6.38)$$

The distance from the phase boundary, which has a temperature T_2 , is h . The temperature at this distance is T_u .

It can be calculated from eq. (6.38) that:

$$T_u^2 = 8 T_2^2 \{1 + 7 \exp(-h/h_0)\}^{-1}, \quad (6.39)$$

with $h_0 = \frac{1}{2} K_c S / 96 \dot{n}_2 T_2^2$, in which K_c/T is the thermal conductivity of the concentrated phase.

Only when $h \ll h_0$ one achieves $T_u \approx T_2$. In our small dilution refrigerator in which we did the experiments with the triple mixing chamber $S = 1 \text{ cm}^2$, $\dot{n}_2 = 20 \text{ } \mu\text{mol/s}$ and $T_2 = 10 \text{ mK}$ one finds $h_0 = 19 \text{ cm}$. The condition $h \ll h_0$ can thus easily be satisfied in the low temperature region.

Conclusions.

It is convenient to rewrite the equations describing the double mixing chamber in reduced form. The reduced temperatures are then only functions of the heating power q_2 and the dimensionless parameter A_1 . Hence all possible configurations of the double mixing chamber can be plotted in one graph (fig. 6.3).

The temperature of the incoming ^3He (T_i) hardly changes when a single mixing chamber is replaced by a multiple mixing chamber, because the exit temperature (T_e) is only a fraction higher than the exit temperature of a single mixing chamber.

The comparison of dilution refrigerators with a single and with

a double mixing chamber shows that it is advisable, for reasons of cooling power, economy and space, to employ a double mixing chamber instead of a single mixing chamber in several cases. The triple mixing chamber, in stationary state, can be described with equations analogous to those of a double mixing chamber. It is however important to choose the distance from the phase boundary to the concentrated line to MC3 small enough (eq. (6.39)).

References.

- Coops, G.M., Waele, A.Th.A.M. de and Gijsman, H.M., *Cryogenics* 19 (1979) 659.
- Frossati, G., Godfrin, H., Hébral, B., Schumacher, G. and Thoulouze, D., *Proc. Hakone, Int. Symp., Japan* (1977), ed. T. Sugawara (1978, Phys. Soc. of Japan) p. 205.
- Frossati, G., Hébral, B., Schumacher, G. and Thoulouze, D., *Cryogenics* 18 (1978) 277.
- Polturac, E. and Rosenbaum, R., *Proc. Hakone, Int. Symp., Japan* (1977), ed. T. Sugawara (1978, Phys. Soc. of Japan) p. 274.
- Polturac, E., Rosenbaum, R. and Soulen, R.J. jr., *Cryogenics* 19 (1979) 715.
- Schumacher, G., thesis, Faculté des Sciences U.S.M.C., Grenoble 1978.
- S.H.E., compagny, private communication.
- Waele, A.Th.A.M. de, Reekers, A.B. and Gijsman, H.M., *Proc. ICEC 6, IPC Science and Technology Press* (1976) p.112.
- Waele, A.Th.A.M. de, Reekers, A.B. and Gijsman, H.M., *Physica* 81B (1976a) 323.
- Waele, A.Th.A.M. de, Reekers, A.B. and Gijsman, H.M., *Proc. 2nd Int. Symp. on Quantum Fluids and Solids, Sanibel Island, Fla., USA* (1977), ed. Trickey, Adams and Dufty (1977, Plenum Publ. Cy.) p. 451.

in our large dilution refrigerator is given. The system consists of a relatively small mixing chamber MC1 and a larger mixing chamber MC2. The volume of the first mixing chamber is about 14 cc. The volume of the concentrated phase in MC1 is about 7 cc. The total volume of the second chamber is 191 cc with a concentrated phase volume of 10 cc. All tubes were calculated as described in chapter IV and chapter VI.

The temperatures in the system were measured with CMN thermometers. The temperature of the ^3He leaving the last heat exchanger was measured by thermometer CMN-T₁. This temperature can be increased by a heater H₁ situated before the last heat exchanger to avoid large temperature gradients near the thermometers and the DMC system. The temperature of the concentrated ^3He leaving the first mixing chamber (MC1) is measured by CMN-T₁. The level of the phase boundary is measured by a capacitive method which will be described in section 7.10.

The part \dot{n}_1 diluted in MC1 flows through Z₁ and its temperature after passing this impedance is measured by CMN-T₃.

The precooled concentrated ^3He (\dot{n}_2) flows, through a heater H₂ which will be described in section 7.4, into the second mixing chamber.

This mixing chamber is surrounded by a shield of μ -metal. In MC2 an araldite platform (thickness about 2 mm) was installed to reduce eventual temperature gradients in the lower part of the mixing chamber (Ch. VI and Masafumi Kumano, 1979). On this platform a capacitor C₂, a heater of manganin wire (H₃), a CMN thermometer (CMN-T₂) and the NBS Superconducting Fixed Point Device are mounted. The capacitor C₂ measures the level of the phase boundary. With the heater H₃ it is possible to supply heat directly into the mixing chamber.

The heater H₄ offers the possibility to supply heat to the exit tube of MC2.

Before the diluted flows \dot{n}_1 and \dot{n}_2 mix, their temperatures are measured with CMN-T₃ and CMN-T₄. After mixing, the temperatures of the diluted ^3He leaving the total DMC system were measured with CMN-T_e.

7.3 The experimental procedure.

Before installing the radiation shield at room temperature the μ -metal shield around the second mixing chamber is demagnetised by applying an ac magnetic field, which is subsequently slowly reduced to zero. In this way the magnetic field inside the mixing chamber is reduced to acceptable values, this because of the sensitivity for magnetic fields of the NBS device (NBS, 1979). With the NBS device we calibrated all thermometers in the second mixing chamber successively. During calibration not only the CMN in question but also the entire holder and the coils are inside the mixing chamber. When the thermometers, calibrated in this way, are used to measure the temperatures T_1 , T_2 , T_3 , T_4 and T_e only the CMN is in the liquid with the coil system in vacuum, as can be seen from fig. 7.1. In principle it is possible that temperature gradients exist in the thermometer which will lead to a difference between the temperature of the liquid and the indicated temperature. The temperature is calculated from $T = C/(V - V_\infty)$ (Ch. III), with C a calibration constant, V the measured voltage at temperature T and V_∞ the voltage deduced from the 4.2 K value. Changes of the thermometers may give deviations of C and V_∞ . This can be noted e.g. from the values measured at 4.2 K. Especially at higher temperature ($T \approx 100$ mK) errors go up to about 15%. At lower temperatures this error decreases to about 4% at 20 mK. However, when the thermometers are not displaced, we find a good reproducibility (in the order of 1%) in the value at 4.2 K. All measurements given in this chapter are performed with the dilution refrigerator in a stationary state. After a change in heating power or flow rate it took about 1 hour to reach equilibrium. To measure different values of the impedance (Z_1) we changed the dilute exit tube of the first mixing chamber. It took about 1 week to change the impedance and to perform a set of measurements.

7.4 Cooling power measurements.

When measuring the cooling power it is important to define in which way the temperature is measured and how the heat is supplied to the system. This statement will be explained by the following experiments.

In the first experiment, with a flow rate of $\dot{n}_1 \approx 0.5$ mmol/s, the

heat was supplied directly to a single mixing chamber with heater H_3 and also with a heater H_4 fixed at the exit tube. The cooling power curves measured with these heaters are identical (a surprising result) and are plotted in fig. 7.2. The cooling power at high

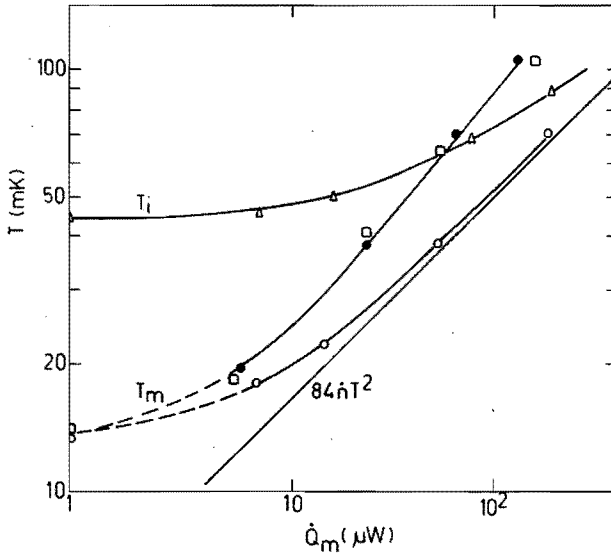


Fig. 7.2 The cooling power of a single mixing chamber with a total flow rate of $\dot{n}_i \approx 0.5$ mmol/s and with several heaters:

- H_2 , heater fixed at input line of the mixing chamber (large surface);
- H_3 , heater inside MC2;
- H_4 , heater fixed at exit tube;
- △ temperature (T_i) of the ^3He leaving the last heat exchanger.

temperatures should be equal to $84 \dot{n}_i T_m^2$ as follows from eq. (6.5), because the inlet and outlet temperatures become equal. However, the cooling power measured with H_3 and H_4 is too small at high temperatures. Presumably the heat produced in H_3 and H_4 causes large temperature gradients because their surface areas are small. It is possible that a small fraction of the heat produced in these heaters flows via the CMN into the liquid, resulting in an apparent

extra temperature increase of the liquid. In order to avoid this effect we have enlarged the contact surface area of the heater with the liquid in the following way. We installed three sintered copper heat exchangers each with a surface area of about 0.5 m^2 in the input line of the mixing chamber (fig. 7.1). Around the middle heat exchanger we wrapped a manganin wire and impregnated it with GE 7031 varnish. The other exchangers were installed to make sure that all heat produced in this heater (H_2) flows into the liquid and not to the other parts in the system. All cooling power measurements reported in this thesis are performed with this arrangement.

In fig. 7.2 also the cooling power of a single mixing chamber while heating in H_2 is given. At high temperatures it is indeed equal to the theoretical value $84 \dot{n}_1 T_m^2$. All measurements on a single mixing chamber with heater H_2 are in agreement with eq. (6.5) while the data with H_3 and H_4 are not.

In fig. 7.3 cooling power measurements of MC2 of a double mixing

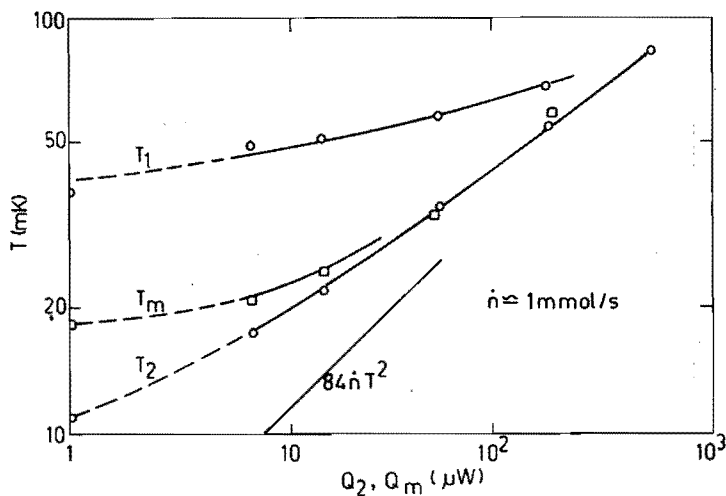


Fig. 7.3 The measured cooling power of a DMC (T_2) and of a SMC (T_m) with a flow rate $\dot{n}_i \approx 1 \text{ mmol/s}$, $Z_1 = 0.31 \times 10^{12} \text{ m}^{-3}$. T_1 is the temperature of the first mixing chamber. The temperatures are fitting the equation $T_1 \geq T_m \geq T_2$.

chamber are given for a total flow rate $\dot{n}_1 \approx 1$ mmol/s and an impedance $Z_1 = 0.31 \times 10^{12} \text{ m}^{-3}$. For the temperatures of this system we find $T_1 \geq T_m \geq T_2$ which agrees with eq. (6.8).

It should be noted that the temperature reduction between the first mixing chamber and the second mixing chamber for $\dot{Q}_2 = 0$ is about 20% higher than the expected value of 2.8. A temperature reduction larger than 2.8 was also reported by Wheatley (1971).

Also for the triple mixing chamber we measured the cooling power. These experiments were executed in our small dilution refrigerator. As an example the results are given for a flow rate of $28 \mu\text{mol/s}$, no heat input on the first and second mixing chamber and $Z_1 = 12 \times 10^{12} \text{ m}^{-3}$ and $Z_2 = 5 \times 10^{12} \text{ m}^{-3}$ (fig. 7.4).

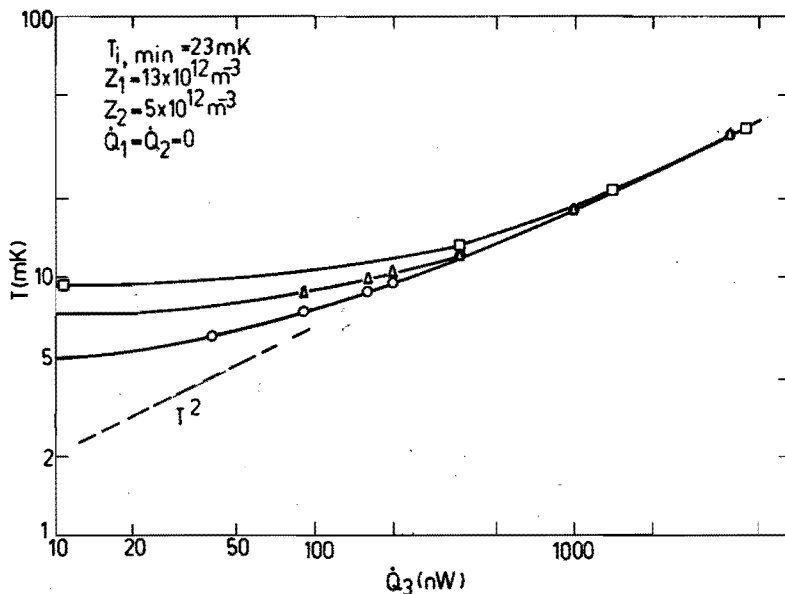


Fig. 7.4 The measured cooling power of a triple mixing chamber. The minimum temperature in this geometry was 4 mK with a total flow rate $\dot{n}_i \approx 28 \mu\text{mol/s}$. Also the cooling power of a single mixing chamber (SMC) is given. $\circ = \text{MC3}$, $\Delta = \text{MC2}$, $\square = \text{SMC}$.

The lowest temperature measured in the small dilution refrigerator with a triple mixing chamber system was 3.0 mK. The total flow

was $\dot{n}_i = 21 \mu\text{mol/s}$ and the impedance $Z_1 = 17 \times 10^{12} \text{ m}^{-3}$ and $Z_2 = 5.1 \times 10^{12} \text{ m}^{-3}$.

The determination of the low temperature limit of the large dilution refrigerator will be part of further investigations.

7.5 The t_2 vs. q_2 measurements.

From the measured T_i , T_2 , \dot{n}_i , \dot{Q}_2 values and the value of Z_1 determined at room temperature one can calculate the dimensionless parameters A_1 , t_1 , t_2 and q_2 from eq. (6.12).

In fig. 7.5 a plot of t_2 vs. A_1 for $Z_1 = 1.5 \times 10^{12} \text{ m}^{-3}$ and $Z_1 = 12.3 \times 10^{12} \text{ m}^{-3}$ and for several flow rates ($\dot{n}_i = 0.5, 1.0, 1.5 \text{ mmol/s}$) is given. From this plot and fig. 6.3a one can derive

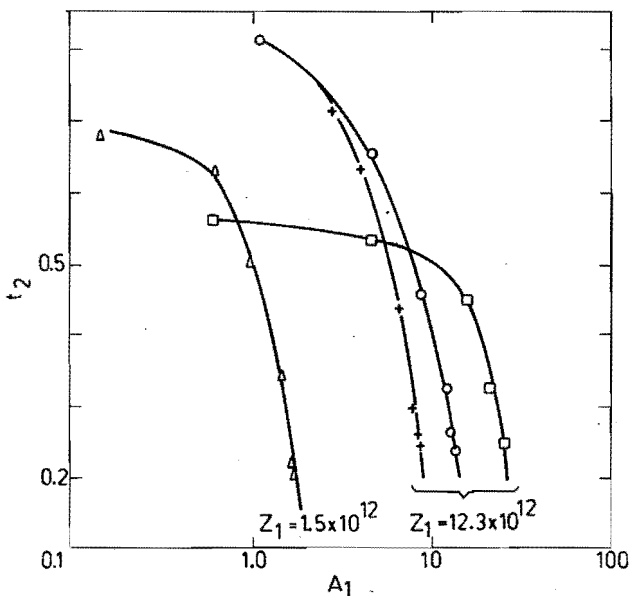


Fig. 7.5 t_2 vs. A_1 with $Z_1 = 1.5 \times 10^{12} \text{ m}^{-3}$ and $Z_1 = 12.3 \times 10^{12} \text{ m}^{-3}$ for several flow rates.

\square $Z_1 = 12.3 \times 10^{12} \text{ m}^{-3}$ $\dot{n}_i = 0.5 \text{ mmol/s}$
 \circ $Z_1 = 12.3 \times 10^{12} \text{ m}^{-3}$ $\dot{n}_i = 1.0 \text{ mmol/s}$
 $+$ $Z_1 = 12.3 \times 10^{12} \text{ m}^{-3}$ $\dot{n}_i = 1.5 \text{ mmol/s}$
 Δ $Z_1 = 1.5 \times 10^{12} \text{ m}^{-3}$ $\dot{n}_i = 1.0 \text{ mmol/s}$

the corresponding theoretical t_2 vs. q_2 curves and compare this with the measured (t_2 , q_2) values. In fig. 7.6 the corresponding

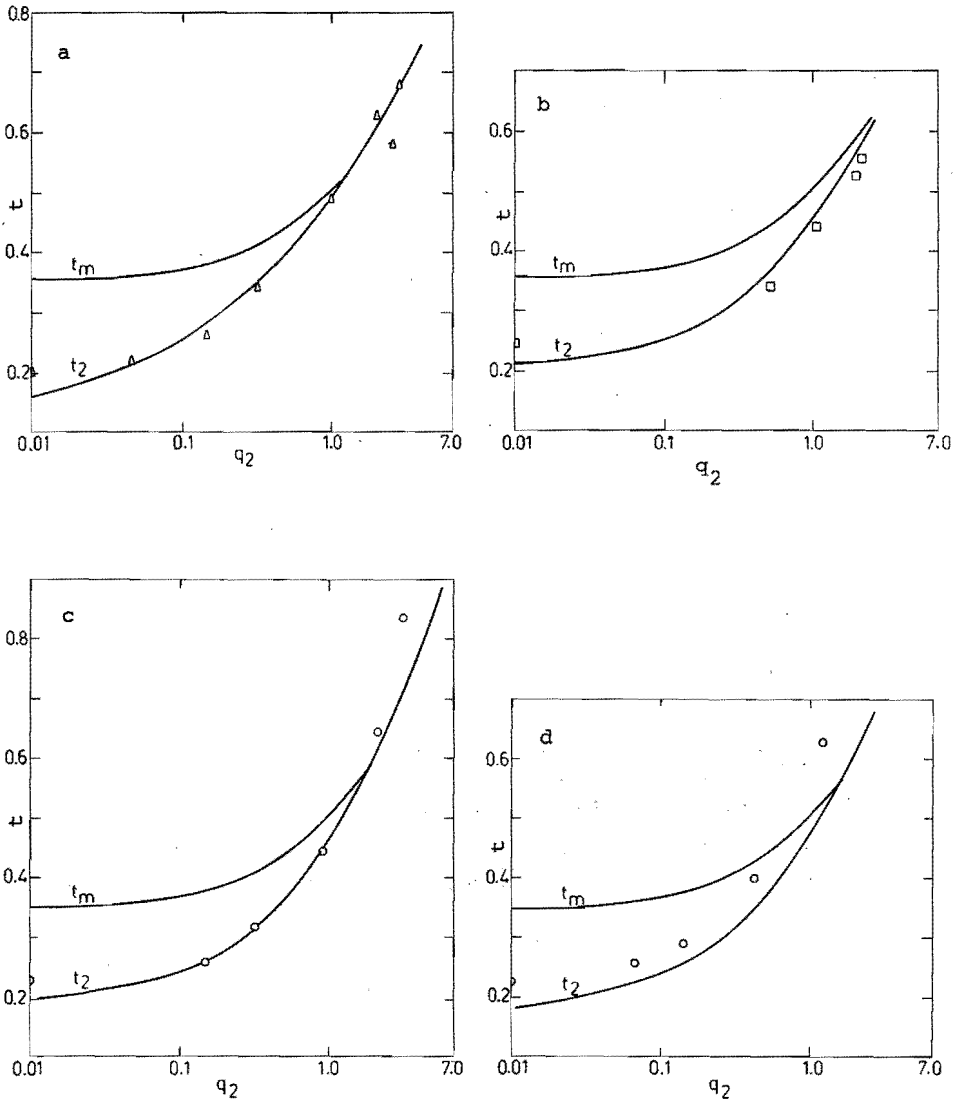


Fig. 7.6 t vs. q_2 for a double and a single mixing chamber with several Z_1 and \dot{n}_i values.

The lines are the theoretical curves derived from the measured A_1 .

- a) $Z_1 = 1.5 \times 10^{12} \text{ m}^{-3}$ $\dot{n}_i \approx 1.0 \text{ mmol/s}$
- b) $Z_1 = 12.3 \times 10^{12} \text{ m}^{-3}$ $\dot{n}_i \approx 0.5 \text{ mmol/s}$
- c) $Z_1 = 12.3 \times 10^{12} \text{ m}^{-3}$ $\dot{n}_i \approx 1.0 \text{ mmol/s}$
- d) $Z_1 = 12.3 \times 10^{12} \text{ m}^{-3}$ $\dot{n}_i \approx 1.5 \text{ mmol/s}$

theoretical curves and the measured values are given. For flow rates up to 1 mmol/s a good agreement with the theory in Ch. VI is obtained.

For the higher flow rates ($\dot{n}_1 \approx 1.5$ mmol/s) a larger amount of ^4He is circulated with the ^3He . This amount of ^4He effects the cooling power of the refrigerator.

These experiments have been performed with several impedances, each giving similar results. It should be noted that all curves in fig. 7.6 practically coincide. This is due to the fact that the minimum temperature of the double mixing chamber is almost independent of the flow and the value of the impedance Z_1 (see fig. 6.3). At high temperatures the curves are also identical because then the double mixing chamber behaves as a single mixing chamber. To show this effect also the calculated values of a single mixing chamber, according to eq. (6.13) $1 + q_m = 8 t_m^2$, are given in fig. 7.6. The reduced cooling power q_2 has a maximum value $q_2 = 7$ corresponding with $Q_2 = 84 \dot{n}_1 T_2^2$. This is also indicated in fig. 7.6.

7.6 The t_1 vs. q_2 measurements.

In the same way as described in section 7.5 we plotted the calculated and measured t_1 vs. q_2 dependences. A typical result is given in fig. 7.7. The temperature of the first mixing chamber

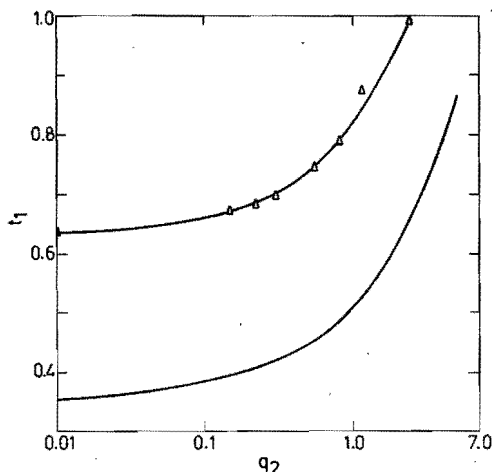


Fig. 7.7 A typical measured t_1 vs. q_2 curve for a double mixing chamber with $Z_1 = 0.31 \times 10^{12} \text{ m}^{-3}$ and $\dot{n}_i \approx 0.5$ mmol/s. The lowest curve is calculated.

is much higher than expected. Since the t_2 - q_2 dependence is well described by the theory we assume that thermometry problems cause this effect. Measurements were performed at the concentrated exit tube and at the bottom of MC1 both giving the same result.

As is shown in section 7.4 the ratio between the first and second mixing chamber is larger than 2.8. It could be that effects, more fundamental than thermometric errors, cause this deviation. It is advisable to proceed with the research on this subject.

7.7 The dependence of A_1 and t_2 on T_i .

According to eq. (6.12) the parameter A_1 varies quite rapidly with the temperature T_i of the ^3He leaving the last heat exchanger. This temperature can be changed by the heater H_1 situated before the last heat exchanger. In this way it is possible to change A_1 without changing Z_1 or the flow rate \dot{n}_i . In fig. 7.8 measurements with a flow rate $\dot{n}_i \approx 1$ mmol/s and with two different Z_1 values are plotted. We note that A_1 is large at low temperatures and small at high temperatures.

In the region where the temperatures of the incoming ^3He were rather high ($T_i > 80$ mK), the parameter η_d cannot be considered

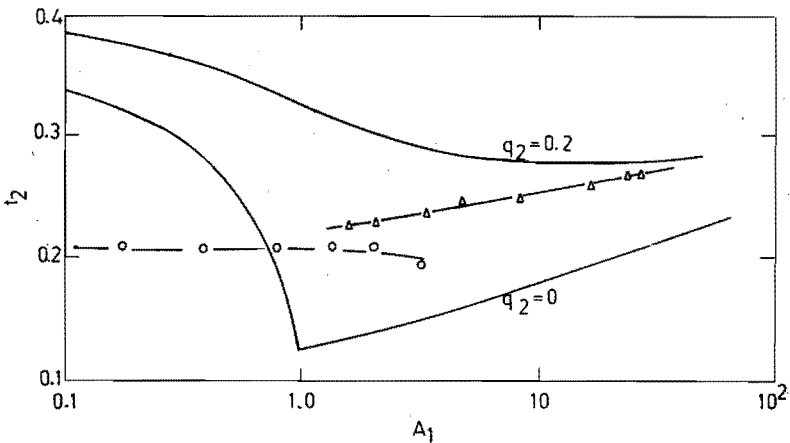


Fig. 7.8 t_2 vs. A_1 measurements for two different Z_1 values. A_1 is changed by changing the temperature (T_i) of the ^3He leaving the last heat exchanger.

The flow rate $\dot{n}_i \approx 1$ mmol/s, $\dot{Q}_1 = \dot{Q}_2 = 0$.

$\Delta Z_1 = 12.3 \times 10^{12} \text{ m}^{-3}$.

$\circ Z_1 = 1.5 \times 10^{12} \text{ m}^{-3}$.

as temperature independent. In this situation large corrections (up to a factor 6) must be used. These corrections (or the real viscosity) can be deduced from the measurements of Kuenhold et al. (1974) and have been taken into account in fig. 7.8. The measured $t_2 - A_1$ values deviate from the theoretical curves. Probably amounts of ^3He enter the second mixing chamber periodically as the result of an instability.

7.8 The dependence of the minimum temperature on Z_1 .

According to the theory the minimum temperature of the second mixing chamber (which is the temperature T_2 with $\dot{Q}_2 = 0$ for a given geometry and flow rate) should hardly depend on the value of Z_1 (fig. 6.3).

In fig. 7.9 the minimum temperature as a function of the impedance Z_1 (measured at room temperature) is given for two different flows ($\dot{n}_1 = 0.5, 1.0$ mmol/s). The curves have a rather flat minimum.

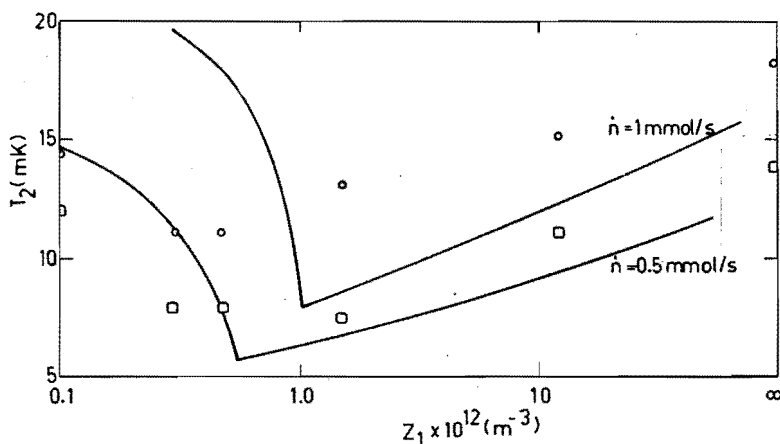


Fig. 7.9 The measured minimum temperature ($\dot{Q}_1 = \dot{Q}_2 = 0$) as a function of the impedance Z_1 for two different flows: $\circ \approx 1$ mmol/s and $\square \approx 0.5$ mmol/s. The values for $Z = \infty$ are the values of a SMC. The lines represent the theoretical curves for $\dot{n}_i \approx 1$ mmol/s ($T_i = 65$ mK) and $\dot{n}_i \approx 0.5$ mmol/s ($T_i = 46$ mK).

This minimum is situated at about $0.3 \times 10^{12} \text{ m}^{-3} \leq Z_1 \leq 1.0 \times 10^{12} \text{ m}^{-3}$ or $0.3 \leq A_1 \leq 0.8$ for $\dot{n}_1 = 1$ mmol/s and $T_1 = 65$ mK.

For $\dot{n}_i = 0.5 \text{ mmol/s}$ and $T_i = 45 \text{ mK}$ we find
 $0.3 \times 10^{12} \text{ m}^{-3} \leq Z_1 \leq 1.5 \times 10^{12} \text{ m}^{-3}$ and $0.5 \leq A_1 \leq 2.6$. Both
 ranges of values of A_1 are in agreement with the theoretical
 value $A_1 \approx 1$.

At very high impedances ($Z_1 \rightarrow \infty$) and at very low impedances the
 minimum temperature of the DMC approaches the minimum temperature
 of a single mixing chamber.

In fig. 7.10 the measured cooling powers of some DMC configurations

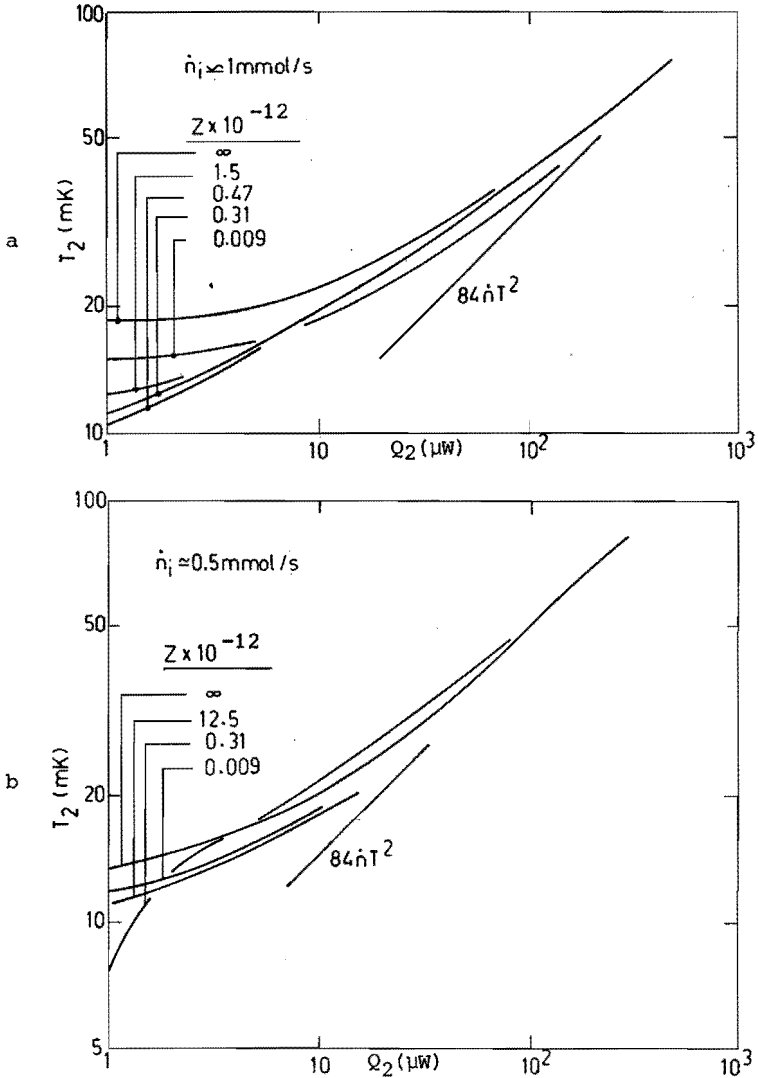


Fig. 7.10 The cooling power of a DMC for $\dot{n}_i \approx 0.5 \text{ mmol/s}$ and
 $\dot{n}_i \approx 1 \text{ mmol/s}$ for several impedances.

with different Z_1 values are given for flow rates of 1 mmol/s and 0.5 mmol/s.

At high temperatures all temperatures tend to the SMC value.

7.9 The dependence of the minimum temperature on the flow rate.

According to the theory $A_1 \sim \dot{n}_i T_i^{-4}$ (eq. (6.12)) and $\dot{n}_i = \alpha T_i^2$ (eq. (4.14)). Hence

$$A_1 \sim \dot{n}_i^{-1}. \quad (7.1)$$

In fig. 7.11 the minimum temperature of the second mixing chamber is given as a function of the total flow rate. The temperature T_1 and also the A_1 values, derived from the measurements of T_i , \dot{n}_i and Z_1 are given.

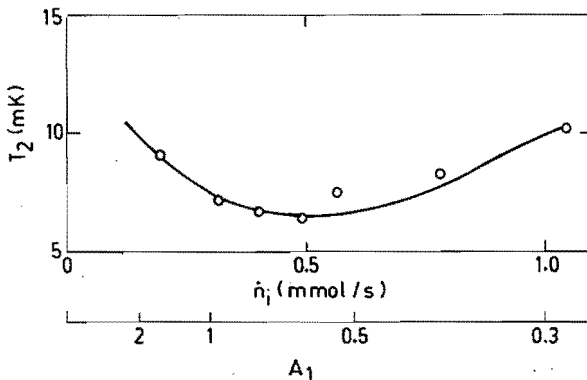


Fig. 7.11 The dependence of the minimum temperature of the second mixing chamber T_2 on the flow rate for $Z_1 = 0.31 \times 10^{12} \text{ m}^{-3}$.

This figure shows that the minimum temperature with $Z_1 = 0.31 \times 10^{12} \text{ m}^{-3}$ is obtained with a flow rate $\dot{n}_i \approx 0.5 \text{ mmol/s}$. This corresponds to $A_1 \approx 0.6$, which is the good order of magnitude.

7.10 Measurements of Δh .

For the measurement of the level difference between the phase boundaries in the first and in the second mixing chamber capacitors are used, one in each mixing chamber. They consist of two concentric cylinders. The outer diameter is 6 mm and the annular

space has a width of 0.5 mm. This width is so large that capillary effects may be neglected.

To avoid raising of the phase boundary due to osmotic pressure differences between the upper and lower part of the mixing chamber a narrow slit (0.5 mm) is machined along the length of the tubes. The values of the capacitors were measured with a General Radio Capacitance bridge (1615A) with a PAR 5101 lock-in amplifier used as a null-detector and oscillator.

The capacitor was calibrated with liquid ^4He at 1 K. The sensitivity was 223 fF/cm in agreement with the value calculated from the dimensions of the capacitor and the dielectric constant of ^4He . From this value the sensitivity for a level change of the phase boundary can be calculated and is $\Delta C/\Delta h \approx 53$ fF/cm.

In fig. 7.12 an "extraction" experiment is plotted. This experiment consists of successively removing small amounts of ^3He from the

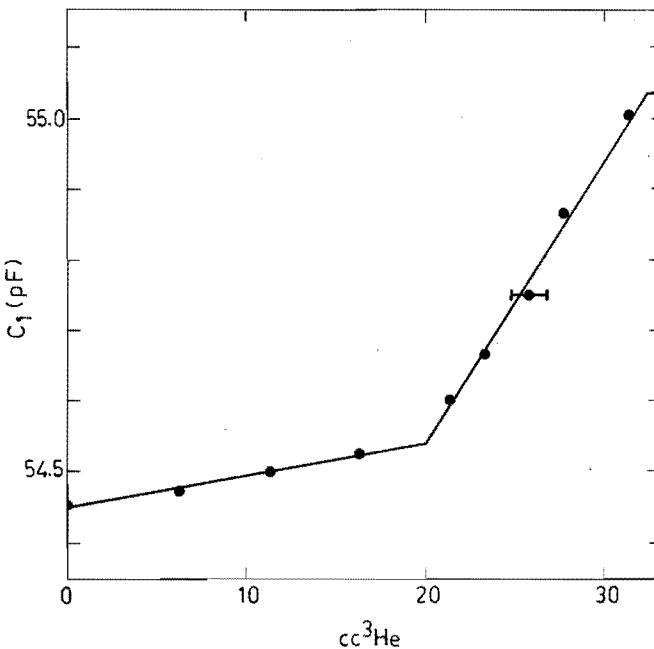


Fig. 7.12 The value of the capacitor in the first mixing chamber. When about 20 cc ^3He is removed from the system the second mixing chamber is empty and at about 30 cc ^3He the first mixing chamber is empty.

dilution refrigerator system. As a result of the raising of the phase boundary the capacitance increases until a final value is reached. At this moment there is no more concentrated ^3He inside the capacitor. From these measurements could be deduced that the capacitor detects the level of the phase boundary properly. The sensitivity of this capacitor can be derived from the slope of curve in fig. 7.12, because we know the surface area of the second mixing chamber ($\approx 10 \text{ cm}^2$). From these measurements we find $\Delta C/\Delta h \approx 48 \text{ fF/cm}$ which is in agreement with the calculated value. The observed level differences are systematically in the range of 0 - 10 mm substantially smaller than the values calculated from eq. (6.20). No satisfactory explanation has been found yet. The value of Δh may be reduced as a result of a pressure drop in Z_c . It should be noted that, apparently, the effects causing a deviation of Δh do not disturb the performance of the double mixing chamber. In the small dilution refrigerator we had indirect evidence that Δh had the correct value. Therefore we are led to the impression that effects associated with the geometry or size of the system are responsible for the small observed Δh value in the large dilution refrigerator.

7.11 The relation between the temperature of MCI and the temperature of the exit of the impedance.

According to section 6.2.5 the temperature (T_3) of the liquid at the exit of the impedance (Z_1) is equal to 1.3 times the temperature (T_1) of the first mixing chamber if $A > 1$ and $\dot{Q}_2 = 0$. In fig. 7.13 the temperature of the ^3He leaving the impedance has been plotted as a function of the temperature of the first mixing chamber for several different impedances and for $\dot{n}_1 \approx 1 \text{ mmol/s}$ and 0.5 mmol/s . To change the temperature of the first mixing chamber H_1 was used so $\dot{Q}_2 = 0$. The slope $dT_3/dT_1 = 1.24$ which is in agreement with the calculations. The values for $Z_1 = 0.009 \times 10^{12} \text{ m}^{-3}$ do not agree with this value. This might be due to the A_1 value (≈ 0.01) which is much smaller than $A_1 = 1$.

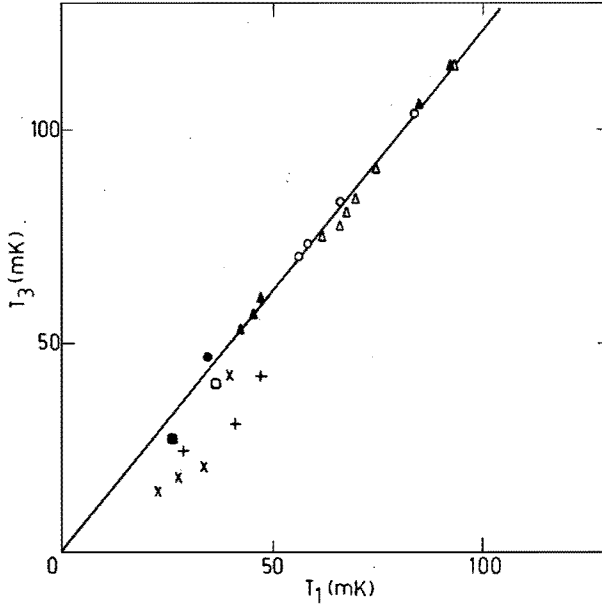


Fig. 7.13 The temperature (T_3) at the exit of the impedance (Z_1) vs. the temperature of the first mixing chamber (T_1) for several Z_1 values. The slope is 1.24 which is in reasonable agreement with the calculations.

$Z \times 10^{12} \text{ m}^{-3}$	1 mmol/s	0.5 mmol/s
0.09	+	x
0.31	□	■
0.47	△	▲
12.5	○	●

7.12 The entrance and exit temperature of a DMC and a SMC.

According to the calculations in section 6.2.5 the entrance temperature (T_1) of a double mixing chamber system should not differ from that of a single mixing chamber under the same conditions.

In fig. 7.14 the entrance (T_1) and the exit temperatures (T_e) for a SMC and for a DMC configuration with $Z_1 = 12.3 \times 10^{12} \text{ m}^{-3}$ are given for a total flow rate $\dot{n}_i \approx 0.5 \text{ mmol/s}$.

The exit temperatures of a single and of a double mixing chamber differ a factor 1.4 at most at the lowest temperature.

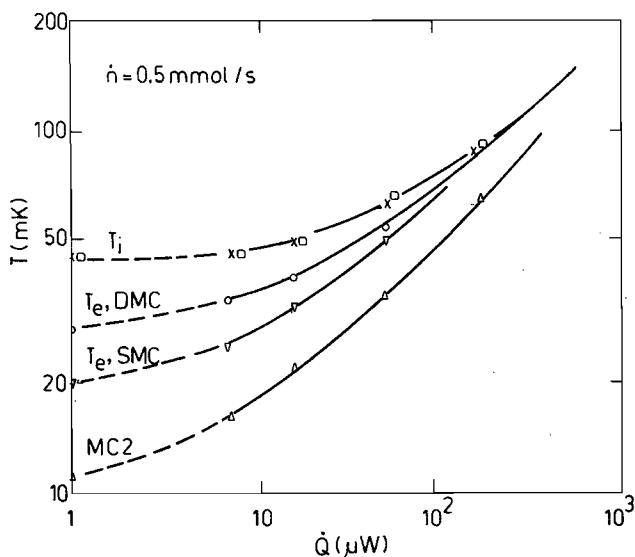


Fig. 7.14 The measured exit (T_e) and entrance (T_i) temperatures with a flow rate $\dot{n}_i = 0.5 \text{ mmol/s}$ vs. the heat supplied to the mixing chamber.

∇ T_e of a SMC.

\circ T_e of a DMC.

\square T_i of a SMC.

\times T_i of a DMC.

Δ temperature of MC2 ($Z_1 = 12.3 \times 10^{12} \text{ m}^{-3}$).

The entrance temperature T_i in both cases is the same. These results are in good agreement with the theory.

Conclusions.

Comparisons of the experiments with the calculations of chapter VI are given. The deviations from the theory of some parameters are not fully understood at the moment. The most important are T_1 and Δh . These deviations do not seem to influence the performance of the double mixing chamber in a negative sense. On the contrary, a small level difference Δh is attractive for the design of a double mixing chamber. The most important parameter from the point of view of the application, the cooling power, is well described by the theory.

Also the dependences of the minimum temperature T_2 on the total flow rate and of the impedance Z_1 agree rather well.

As a final remark we like to note that now several years of experience exist with the multiple mixing chamber. From these experiments we may conclude that the multiple mixing chamber system is a reliable and convenient tool for maintaining temperatures below 4 mK continuously.

References.

- Kuenhold, K.A., Crum, D.B. and Sarwinski, R.E., Proc. LT 13 (1972), Boulder.
- Masafumi Kumano and Yusaku Ikegami, Rev. Sci. Instr. 50 (1979) 24.
- N.B.S. Special Publication 260-2.
- Wheatley, J.C., Rapp, R.E. and Johnson, R.T., J. Low Temp. Phys. 4 (1971) 1.

SUMMARY.

A dilution refrigerator is an instrument to reach temperatures in the mK region in a continuous way. The temperature range can be extended and the cooling power can be enlarged by adding an extra mixing chamber. In this way we obtain a double mixing chamber system.

In this thesis the theory of the multiple mixing chamber is presented and tested on its validity by comparison with the measurements.

Measurements on a dilution refrigerator with a circulation rate up to 2.5 mmol/s are also reported.

Preceding this research we investigated resistance and CMN thermometry. This study confirmed the impression, that one has to be careful with CMN thermometers to prevent eventual dehydration or liquefying, which make the thermometer useless for low temperature measurements. As far as resistance thermometry is concerned we measured the power which is necessary to change the measured temperature 1% from the temperature to be determined.

For the design of heat exchangers and tubes we give theoretical derivations, which are relevant for the construction of dilution refrigerators. We derived that it is necessary to build a larger dilution refrigerator if one wants to reach the temperature region of 2 mK.

In the design of this refrigerator with a large ^3He circulation rate (the large refrigerator) one has to take into account the ^4He evaporation rate of the bath. In order to minimize this effect we paid attention to the heat balance of the refrigerator especially of the part having a temperature between 4 - 80 K.

The pumping system is designed to circulate 4 mmol/s. However, with a ^3He circulation larger than 2.5 mmol/s too much ^4He circulates through the system, which hampers a good operation of the dilution refrigerator. We observed that the large flow impedance of the still orifice causes this effect. It is advisable to change this orifice in the future.

We also measured the cooling power of the large refrigerator with a single mixing chamber. With a ^3He circulation rate of for instance 1 mmol/s and a temperature of 20 mK the measured cooling power is about 8 μW . This is one of the highest cooling powers ever reported. The minimum temperature at this circulation rate is 18 mK.

We present a theory for the multiple mixing chamber. In spite of its simplicity from a constructive point of view, the multiple mixing

chamber is rather complicated to describe theoretically. The thermodynamic and hydrodynamic properties of the liquids are interweaved with each other in a complicated way. We derived equations for the temperatures at several points in the system and for the level difference of the phase boundaries in the two mixing chambers. It turns out that the flow impedance at the dilute exit of the first mixing chamber plays an important role in the system.

We also present measurements on the double mixing chamber. Some results are not in agreement with the theory and no conclusive explanation has been found yet. In the first place the level difference between the phase boundaries of the first and the second mixing chamber is smaller than predicted by the theory and the temperature of the first mixing chamber is higher than expected. Since it is possible that the observations have a fundamental origin, it is advisable to continue the research in this direction.

A good agreement with theory has been found for the temperature of the second mixing chamber as a function of the power supplied to this mixing chamber. This cooling power has a weak dependence on the flow impedance and the ^3He circulation rate, which is in agreement with the calculations. It is also confirmed that the temperature of the ^3He flowing from the heat exchanger to the mixing chamber is not influenced by changing a single mixing chamber by a double mixing chamber. The temperature leaving the total system is, as has been calculated, somewhat higher than with a single mixing chamber.

The minimum temperature so far of the large refrigerator is 6.5 mK at a flow rate of 0.5 mmol/s. The determination of the low temperature limit of the large dilution refrigerator is suggested to be part of further investigations. In a small dilution refrigerator with a triple mixing chamber and a circulation rate of 28 $\mu\text{mol/s}$ we succeeded to reach 3 mK.

The work of this thesis is part of a research program in which several years of experience with the multiple mixing chamber are reported. We conclude that the multiple mixing chamber is a reliable and convenient tool for lowering the minimum temperature and to increase the cooling power of a dilution refrigerator.

SAMENVATTING.

Een mengkoeler is een instrument om continu temperaturen in het millikelvingebied te bereiken. Het temperatuurbereik kan worden uitgebreid en het koelvermogen worden vergroot in het lage temperatuurgebied door de toevoeging van een tweede mengkamer in de bestaande mengkoeler. Aldus ontstaat de dubbele mengkamer.

In dit proefschrift wordt de theorie van de meervoudige mengkamer gepresenteerd en aan de hand van metingen op haar juistheid getoetst. Tevens worden de metingen aan een mengkoeler met een ^3He circulatie tot 2,5 mmol/s gegeven.

Voorafgaande aan dit onderzoek is aandacht besteed aan de weerstands- en CMN thermometrie. Deze studie bevestigde de indruk, dat CMN thermometers met zorg behandeld dienen te worden. Er moet voor gewaakt worden, dat zich ontwatering of vervloeiing voordoen, die de thermometer voor meting van lage temperaturen onbruikbaar zouden maken. Ten aanzien van de weerstandsthermometrie werd voor verschillende thermometers het vermogen bepaald waarbij de aangegeven temperatuur 1% van de te bepalen temperatuur afweek.

Voor het ontwerpen van warmtewisselaars en buizen worden uitdrukkingen afgeleid, die in het algemeen bij het bouwen van mengkoelers van belang zijn. Aangetoond wordt, dat het noodzakelijk is om een grote mengkoeler te bouwen als men temperaturen van circa 2 mK continu wil bereiken. Bij de bouw van deze mengkoeler met een hoge ^3He circulatie (verder de grote mengkoeler genoemd) dient ook rekening te worden gehouden met het ^4He -verbruik van het bad. Teneinde dit te minimaliseren is aandacht besteed aan de warmtehuishouding van de mengkoeler, speciaal van dat gedeelte dat temperaturen heeft tussen 4 en 80 K. Het pompsysteem van deze machine is ontworpen voor een ^3He circulatiesnelheid van 4 mmol/s. Het bleek echter dat bij een totale circulatie boven 2,5 mmol/s teveel ^4He mee circuleerde, wat een goede werking van de mengkoeler belemmert. Gebleken is dat de grote stromingsweerstand van het verdamper-diafragma hiervan de oorzaak is. Voor de hand ligt dit diafragma in de toekomst te veranderen.

Het koelvermogen van de grote mengkoeler met een enkele mengkamer is gemeten en is in overeenstemming met de theorie. Bij een ^3He -circulatie van bijvoorbeeld 1 mmol/s en een mengkamertemperatuur van 20 mK is het gemeten koelvermogen ongeveer 8 μW . Dit behoort tot de hoogste

gerapporteerde koelvermogens van een mengkoeler. De minimum temperatuur bij deze circulatie is 18 mK.

Het meervoudig mengkamersysteem wordt theoretisch behandeld. Ondanks zijn eenvoud in constructief opzicht, blijkt de dubbele mengkamer in theoretisch opzicht een gecompliceerd geheel te zijn. Thermodynamische en hydrodynamische (superfluïde) eigenschappen van de vloeistoffen zijn op gecompliceerde wijze met elkaar verweven. Er worden vergelijkingen afgeleid voor de temperaturen op de verschillende plaatsen in het systeem en voor het niveauverschil tussen de fasegrenzen in de twee mengkamers. Het blijkt, dat de stromingsimpedantie in de uitstroompip van de eerste mengkamer een belangrijke rol speelt.

Metingen aan de dubbele mengkamer worden beschreven. Er blijken enkele resultaten niet in overeenstemming met de theorie te zijn en hiervoor is nog geen afdoende verklaring gevonden. Dit betreft in de eerste plaats het hoogteverschil tussen de fasegrenzen in de eerste en de tweede mengkamer, dat kleiner is dan verwacht, en de temperatuur van de eerste mengkamer, die hoger is dan verwacht. Omdat het mogelijk is, dat bij beide genoemde afwijkingen een fundamentele oorzaak bestaat, verdient het aanbeveling het onderzoek op dit gebied voort te zetten. Goede overeenstemming met de theorie is gevonden voor de temperatuur van de tweede mengkamer als functie van het aan deze mengkamer toegevoerde vermogen. Dit koelvermogen blijkt zwak afhankelijk te zijn van de waarde van de stromingsimpedantie en de ^3He -circulatiesnelheid, wat in overeenstemming is met de theorie.

Tevens werd bevestigd, dat de temperatuur van het ^3He , dat uit de warmtewisselaars naar de mengkamer stroomt, niet wordt beïnvloed als een enkele mengkamer door een meervoudige mengkamer wordt vervangen. De temperatuur van het ^3He , dat het systeem verlaat, is zoals ook de berekeningen aantonen iets hoger dan bij een enkele mengkamer.

De minimum temperatuur, die in de grote mengkoeler met een totale circulatiesnelheid van 0,5 mmol/s is bereikt, is 6,5 mK. Voor de hand ligt de bepaling van de laagste temperatuur, die met dit apparaat valt te bereiken, verder te onderzoeken. In een kleinere mengkoeler is het ons gelukt met een drievoudige mengkamer een temperatuur van 3 mK te bereiken bij een circulatiesnelheid van 28 $\mu\text{mol/s}$.

Het werk in dit proefschrift beschreven maakt deel uit van een onderzoek, waarbij nu enkele jaren ervaring met de meervoudige

mengkamer is opgedaan. Uit deze ervaringen kunnen we concluderen, dat de meervoudige mengkamer een betrouwbaar en geschikt instrument is om de minimum temperatuur te verlagen en het koelvermogen van een mengkoeler te vergroten.

SOME QUANTITIES USED IN THIS THESIS.

C_{3c}	$= 24 T$	$T < 0.1 K$
C_{3d}	$= 108 T$	$T < 0.04 K$
H_{3c}	$= 12 T^2$	$T < 0.1 K$
H_{3d}	$= 96 T^2$	$T < 0.04 K$
H_{π}	$= 54 T^2 + 42 T_m^2$	$T_m < T < 0.04 K$
v_c	$= 37 \times 10^{-6}$	$T < 1 K$
v_d	$= 430 \times 10^{-6}$	$T < 0.05 K$
η_c	$= 2 \times 10^{-7} T^{-2}$	$T < 0.1 K$
η_d	$= 0.5 \times 10^{-7} T^{-2}$	$T < 0.05 K$
κ_c	$= 3.3 \times 10^{-4} T^{-1}$	$T < 0.03 K$
κ_d	$= 3.0 \times 10^{-4} T^{-1}$	$T < 0.02 K$
Π	$= 1630 + 10^5 T^2$	$T < 0.1 K$

In this thesis SI units are used, unless otherwise stated.

LIST OF FREQUENTLY USED SYMBOLS.

Subscript c = concentrated phase;

d = diluted phase.

A_k	dimensionless parameter defined in eq. (6.12).
C_{3c}, C_{3d}	molar specific heat of ^3He .
C_1, C_2	capacitor in first and second mixing chamber.
DMC	double mixing chamber.
D	diameter of still orifice.
d_c, d_d	diameter of tube.
d_{sc}, d_{sd}	thickness of sinter sponge
g	gravitational acceleration.
H_{3c}, H_{3d}	molar enthalpy of ^3He .
H_π	molar enthalpy of diluted ^3He at constant osmotic pressure.
Δh	difference in level between the phase boundaries.
L	heat of evaporation.
l_c, l_d	length of tube.
M	molar mass.
MC	mixing chamber
\dot{n}_1, \dot{n}_3	total ^3He flow rate.
\dot{n}_1, \dot{n}_2	flow rate of diluted ^3He in MC1, MC2.
\dot{n}_t	evaporation rate of LHe bath.
\dot{n}_{1K}	flow rate of 1K-bath.
p	pressure.
P	heating power.
\dot{Q}_k	heat supplied to mixing chamber k
q_k	dimensionless heat input parameter of mixing chamber k.
R	electrical resistance.
r	dimensionless flow rate parameter of ^3He diluted in MC1.
R_K	Kapitza resistance coefficient.
SMC	single mixing chamber
S	area
S_{3c}, S_{3d}	molar entropy of ^3He .
T	temperature.
t_k	dimensionless temperature parameter of mixing chamber k.

V_c, V_d	molar volume of ^3He .
Z	flow resistance.
γ	ratio of specific heat capacities.
δ	particle diameter.
ϵ	reduction factor of surface area.
$\eta_c T^{-2}, \eta_d T^{-2}$	viscosity of ^3He .
$\kappa_c T^{-1}, \kappa_d T^{-1}$	thermal conductivity of ^3He .
$\kappa_b T$	thermal conductivity of body material.
Π	osmotic pressure.
$\Pi_o T^2$	temperature-dependent term in the osmotic pressure along the phase separation curve.
$\Delta\rho$	difference in density between the diluted and concentrated phase.
σ_c, σ_d	surface area in heat exchanger.

DANKWOORD.

Op deze plaats wil ik allen die aan dit proefschrift hebben bijgedragen hartelijk danken. Van de velen wil ik er hier enkelen noemen.

Alle leden van de groep Kryogene Technieken, waaronder ir. G.J. v.d. Geest, L.C. van Hout, L.M.W. Penders, en het Kryogeen Bedrijf met J.J.G.M. van Amelsvoort en W.C.T.H. Delissen wil ik hartelijk danken voor hun inzet, ondersteuning en vriendschap, die ik in deze vier en een half jaar ondervonden heb. Zij hebben ervoor gezorgd, dat dit in alle opzichten onvergetelijke jaren zijn geworden. Hierbij wil ik ook alle studenten betrekken, die tijdens mijn aanwezigheid in de groep gewerkt hebben.

Ook zal ik ir. A.B. Reekers niet vergeten, die mij heeft ingewerkt en die vele metingen verrichtte.

T. Satoh contributed a large amount of work especially during the construction and testing period.

Vele leden van de vakgroep Vaste Stof hebben hun medewerking en vriendelijke ondersteuning gedurende deze jaren gegeven.

Het werk had nooit van de grond gekomen zonder de medewerkers van de werkplaatsen, die onder alle omstandigheden voor mij klaar stonden.

Mevr. M.C.K. Gruijters ben ik zeer erkentelijk voor alle tekeningen, die zij zelfs nog op het laatste moment gemaakt heeft.

De medewerkers van de "Lage Temperaturen groep" van het Natuurkundig Laboratorium van de N.V. Philips hebben altijd klaar gestaan als dit nodig was.

Prof.dr. G. Frossati dank ik, dat ik bij hem in Grenoble heb kunnen werken.

Tevens wil ik de Stichting FOM noemen, die mij in de gelegenheid heeft gesteld dit werk te doen.

CURRICULUM VITAE.

- 19-2-1952 Geboren te 's-Gravenhage.
- 1971 Eindexamen Atheneum B.
- 1971-1976 Studie aan de Technische Hogeschool te Delft,
afdeling der Technische Natuurkunde.
Afgestudeerd in de vakgroep Lage Temperaturen onder
leiding van Prof.dr. B.S. Blaisse.
- 1976-1981 Werkzaam aan de Technische Hogeschool te Eindhoven
als wetenschappelijk medewerker in dienst van de
Stichting voor Fundamenteel Onderzoek der Materie,
in de groep Kryogene Technieken onder leiding van
Prof.dr. H.M. Gijsman.
- 1978 Verblijf van 1-2-1978 tot 15-4-1978 te Centre
National de la Recherche Scientifique, Grenoble,
Frankrijk.

STELLINGEN

behorende bij het proefschrift van

G.M. Coops

Eindhoven, 12 juni 1981

1. Het optimale koelvermogen van een meervoudige mengkamer is bij gegeven temperatuur meer dan twee maal zo groot als het optimale koelvermogen van een enkele mengkamer.

Dit proefschrift, hoofdstuk VI.

2. Bij het meten van het koelvermogen dient vermeld te worden waar en hoe de temperatuur gemeten is en op welke wijze het vermogen toegevoerd is.

Dit proefschrift, hoofdstuk VII.

3. Bij het gebruik van CMN thermometers dient men erop bedacht te zijn, dat er vervloeiing of ontwatering op kan treden, die de thermometers onbruikbaar maakt.

Butterworth, G.J., Finn, C.B.P. and Kiyama, K., J. Low Temp. Phys. 15 (1974) 537.

Coops, G.M., Reekers, A.B., Waelle, A.Th.A.M. de and Gijsman, H.M., Proc. ICEC 8, IPC Science and Technology Press (1980) p. 371.

4. De door Okuda en Kadowaki voorgestelde magnetische structuur van $\text{CuCl}_2 \cdot 2\text{NC}_5\text{H}_5$ is aan ernstige bedenkingen onderhevig.

Kiichi Okuda and Kazuo Kadowaki, J. of the Phys. Soc. of Japan, 46 (1979) 45.

5. Het onderzoek aan bouwmaterialen beperkt zich in hoge mate tot het empirisch bepalen van correlaties aan grote proefstukken. Uit oogpunt van kwaliteitsbeheersing en kostenbesparing is een meer fundamentele werkwijze aan te bevelen.

Olszak, W., "Effets cycliques et transitoires dans les structures", Séminaire, Saint-Rémy-Les-Chevreuse (Fr.), oct. 1979.

6. Mullins en Brunnschweiler geven aan, dat beschadiging in de bovenlaag van het silicium van hun gesputterde molybdeen-silicium Schottky-diodes de oorzaak is van de gevonden afwijkingen van het ideale gedrag. Zij gaan daarmee ten onrechte voorbij aan de effecten van geïnduceerde oppervlaktetoestanden, chemisch beschadigde residulagen en de partiële oxidatie van de molybdeenkathode.

Mullins, F.H. and Brunnschweiler, A., Sol. State Electr.
19 (1976) 47.

7. De vroegtijdige vakkensplitsing in het natuuronderwijs miskent de wijze waarop kinderen hun omgeving ervaren. Zij remt de spontaniteit waarmee kinderen vragen stellen en dwingt hen zich te verlaten op de autoriteit van de leraar.
8. Men doet medewerkers tekort door in het dankwoord van een proefschrift uitsluitend hun voornaam te vermelden.
9. De diameter van een dubbeltje wordt steevast te laag geschat.